Green Chemistry

TUTORIAL REVIEW

View Article Online
View Journal | View Issue

Cite this: *Green Chem.*, 2025, **27**, 11312

Catalytic reductive conversion of polyethylene terephthalate (PET) plastic waste into fuels, valuable chemicals and degradable polymers

Jingyu Liu,†[a] Shuyan Yi,†[a,b] Jingwen Cheng[a] and Sibao Liu *[a]

Polyethylene terephthalate (PET) is the most widely used synthetic polyester; however, a significant portion of its waste accumulates in landfills, oceans, and incinerators, posing severe environmental and health risks. Chemical recycling and upcycling are promising solutions for post-consumer PET valorization while mitigating plastic pollution. This review summarizes recent advancements in the catalytic reductive conversion of post-consumer PET into fuels, value-added chemicals, and degradable polymers, with a particular focus on heterogeneous catalysis. The catalytic reductive conversion strategies include hydrogenation, hydrogenolysis, hydrodeoxygenation (HDO), and transfer HDO. A variety of products can be obtained depending on the degree of aromatic ring saturation, ester bond hydrogenation, and C–O bond removal. Reaction pathways for achieving target products are outlined. The performance of the catalysts developed is described and compared in each section. In addition, the role of active sites, structure–activity relationships, and reaction mechanisms are comprehensively discussed. Finally, future perspectives are proposed, with specific emphasis on one-pot tandem processes, non-noble metal catalyst design, the production of new chemicals, the impact of additives, elucidation of reaction networks and mechanistic studies. This review aims to inspire innovative solutions for sustainable PET waste management through advanced catalytic reductive technologies.

Received 18th June 2025,
Accepted 14th August 2025

DOI: 10.1039/d5gc03083h

rsc.li/greenchem

Green foundation

1. This review presents reductive recycling and upcycling strategies, including hydrogenation, hydrogenolysis, HDO, and transfer HDO technologies, as efficient, selective, and versatile routes for converting PET plastic waste into fuels, chemicals, and degradable polymers. These approaches not only address the urgent global demand for plastic valorization but also align with the principles of green chemistry by minimizing waste generation.
2. This review focuses on the reductive conversion of post-consumer PET using heterogeneous catalysis. The roles of active sites, structure–activity relationships, and reaction mechanisms are comprehensively discussed.
3. Future advances will emphasize one-pot tandem processes, non-noble metal catalyst design, pathways for the production of new chemicals, the impact of additives, elucidation of reaction networks, and in-depth mechanistic studies. The proposed perspectives are expected to encourage more efficient reductive process innovation and low-cost catalyst development for sustainable PET waste management, thereby supporting the plastic circular economy.

1 Introduction

Synthetic plastics play a crucial role in our daily lives and their production expanded from 1.5 million tons (Mt) in 1950 to 380 Mt in 2021.[1] However, the manufacture and use of plastics inevitably generate substantial amounts of plastic waste. Most of these plastic wastes are non-degradable and have not been properly managed, ultimately ending up in landfills, oceans, and incinerators, thereby posing severe environmental and human health risks.[2,3] To address the issue of plastic waste, biodegradable plastics, which can partially mitigate plastic pollution, have been developed over the past few decades.[4] Nevertheless, these biodegradable plastics are more expensive than conventional plastics. Moreover, during degradation, these biodegradable plastics release significant amounts of diverse oligomers that exhibit higher bioavailability compared to larger solid plastic particles, thus posing greater exposure risks to wildlife and humans.[5] On the other hand, given that less than 10% of plastic waste has been recycled,[2,6] it is imperative to develop efficient methods to alleviate plastic pollution. In this context, chemical recycling and upcycling, which enable the conversion of plastic waste into fuels, monomers, value-added chemicals, and

[a]*Engineering Research Center of Polymer Green Recycling of Ministry of Education, Fujian Key Laboratory of Pollution Control & Resource Reuse, College of Environmental and Resource Sciences, Fujian Normal University, Fuzhou, Fujian 350007, China. E-mail: liusibao@fjnu.edu.cn*
[b]*International Joint Institute of Tianjin University, Tianjin University, Binhai New City, Fuzhou 350207, China*
†These authors contribute equally to this work.

advanced materials, offer promising solutions for addressing the challenges posed by plastic waste.[7–11]

PET is one of the most commonly used plastics, accounting for approximately 6.2% of annual polymer production.[12,13] The global PET market was valued at $48.43 billion in 2023 and is projected to grow at a compound annual growth rate (CAGR) of 9.5%, reaching $109.63 billion by 2032.[14] Owing to its excellent properties, PET is widely utilized in various applications, including packaging (*e.g.*, water bottles, soft drinks, and food containers), textile fibers, engineering plastics, films and sheets, medical devices, and 3D printing. Despite its importance, the disposal of PET plastic waste has become a growing global concern, as most countries recycle less than 30% on average.[15,16] Consequently, there is an urgent need to develop advanced chemical technologies for the degradation and recycling of PET waste.

Solvolysis including hydrolysis, methanolysis, and glycolysis are the most commonly employed methods for the chemical recycling of PET into monomers such as terephthalic acid (TPA), dimethyl terephthalate (DMT), and bis(2-hydroxyethyl) terephthalate (BHET)[17–24] (Scheme 1). These technologies have been successfully commercialized by several companies, including Carbios, DuPont, Dow Chemicals, Eastman, Teijin, Ioniqa Technologies, Jeplan, and Jiaren New Materials. However, the products obtained through these methods are limited to monomers, which primarily facilitate the establishment of a closed-loop PET recycling pathway. In addition, the solvolysis approach faces several limitations, including: (1) the requirement for a large excess of solvent and degradation agents; (2) the formation of oligomeric side products that are difficult to separate; (3) the use of non-recyclable and corrosive catalysts; and (4) very limited product diversity. Developing more promising approaches for the selective conversion of waste PET into fuels, value-added chemicals, and biodegradable polymers deserves particular attention. Such technologies not only enable the upcycling of PET into higher-value products but also broaden the range of products essential for daily life.

Reductive conversion is one of the emerging technologies capable of transforming PET into a wide range of products. PET is a polymer composed of repeating ($C_{10}H_8O_4$) units linked by ester groups. Through reductive conversion strategies, the benzene ring can be saturated, the ester groups can be hydrogenated, or the C–O bonds can be cleaved. In addition, the scission of C–O bonds in ester groups can occur *via* either the acyl C–O bond or the alkyl C–O bond. Depending on the extent of benzene ring saturation, ester group hydrogenation, and C–O bond removal, various products can be generated. For instance, the full and partial hydrogenation of aromatic rings yields polyethylene-1,4-cyclohexanedicarboxylate (PECHD)[25,26] and polyethylene terephthalate–polyethylene-1,4-cyclohexanedicarboxylate (PET-PECHD),[27] respectively. These polymers are biodegradable. The tandem hydrogenation of aromatic rings and hydrogenolysis of ester groups produces 1,4-cyclohexanedimethanol (CHDM),[28] a valuable monomer for synthesizing advanced functional polyesters. Partial and full HDO of PET generates aromatics and cycloalkanes,[29,30] which can serve as fuel components and building-block chemicals in the chemical industry. Compared to traditional methods, the reductive transformation strategy offers several advantages, including: (1) the ability to produce a diverse range of valuable products that cannot be obtained through solvolysis-based recycling processes; (2) high selectivity toward target products; (3) the use of recyclable heterogeneous catalysts; and (4) mild reaction conditions, even under solvent-free conditions, which enhance the feasibility for practical applications. Therefore, by considering PET waste as a resource, reductive conversion strategies offer numerous possibilities for converting PET into high-value products and represent a promising technology for the upcycling of PET wastes (Scheme 1).

Given the increasing attention paid to this reductive conversion technology in recent years, in this review, we summarize recent advancements in the catalytic reductive conversion of post-consumer PET into valuable products, including fuels, high-value chemicals, and degradable polymers, with a particular focus on heterogeneous catalysis. Key strategies such as hydrogenation, hydrogenolysis, HDO, and transfer HDO are exemplified, along with their respective reaction pathways for achieving target products. The performance of various catalysts is systematically summarized and compared, while the roles of active sites, structure–activity relationships, and underlying reaction mechanisms are comprehensively discussed. Finally, future research directions and challenges in this field are outlined. Over the past five years, a considerable number of high-quality reviews on the chemical recycling of PET have been published.[18–24] These reviews primarily emphasize various depolymerization methods, products, and catalysts, particularly on the solvolysis of PET to monomers. In contrast, this review focuses on catalytic reductive conversion as a versatile approach for transforming PET into a wide range of valuable products, especially *via* heterogeneous catalysis. By examining emerging strategies and mechanistic insights, this review aims to inspire innovative solutions for sustainable PET waste management through advanced reductive catalytic technologies.

2 Hydrogenation of PET to yield biodegradable PECHD or PET-PECHD polyesters

Full and partial hydrogenation of the aromatic rings in PET without depolymerization can yield PECHD and PET-PECHD, respectively (Scheme 2). Both polyesters are biodegradable. Moreover, PECHD exhibits enhanced thermal stability with a melting point approximately 5–10 °C higher than that of PET due to the substitution of an aliphatic ring instead of the aromatic ring.[31,32] Meanwhile, PET-PECHD demonstrates comparable thermal stability and mechanical strength to PET, while also exhibiting superior extensibility and barrier properties.[27] Therefore, the hydrogenation of PET to yield PECHD or PET-PECHD represents a promising approach for the upcycling of PET waste. The primary challenge in this reaction lies in achieving the selective saturation of aromatic rings while preserving the integrity of the ester bonds to prevent depoly-

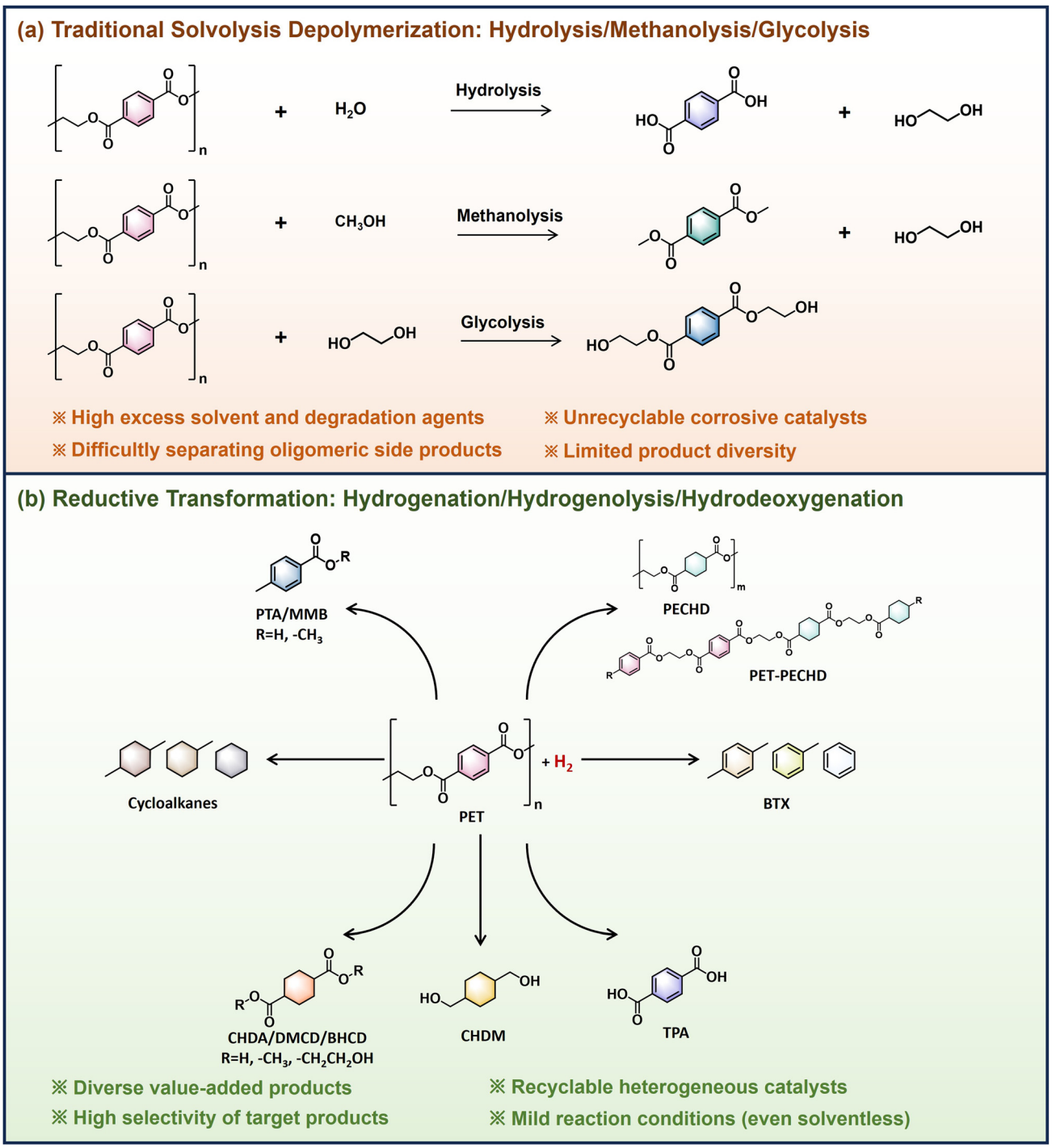

Scheme 1 A comparison of the traditional solvolysis method (a) and reductive transformation (b) for the valorization of PET to fuels, chemicals and polymers.

merization. Noble metal catalysts, such as Ru–Pt bimetallic catalysts[25,26] and the Ru/C catalyst,[27] have been reported as effective options for this strategy. The synergistic effect of the bimetallic catalysts and the on-water hydrogenation mechanism play a crucial role in achieving high hydrogenation activity under mild reaction conditions. The performances of all related catalysts are summarized in Table 1.

Tan *et al.* pioneered the full hydrogenation of PET to PECHD using Rh–Pt bimetallic catalysts in 1,1,1,3,3,3-hexafluro-2-propanol (HFIP) or water as solvents.[25,26] Specifically, when HFIP was employed as the solvent, a Vulcan XC-72 carbon-supported Rh–Pt catalyst effectively catalyzed the complete hydrogenation of PET to PECHD under mild reaction conditions (50 °C, 6.89 MPa H_2 for 1 h). The polyol synthesis

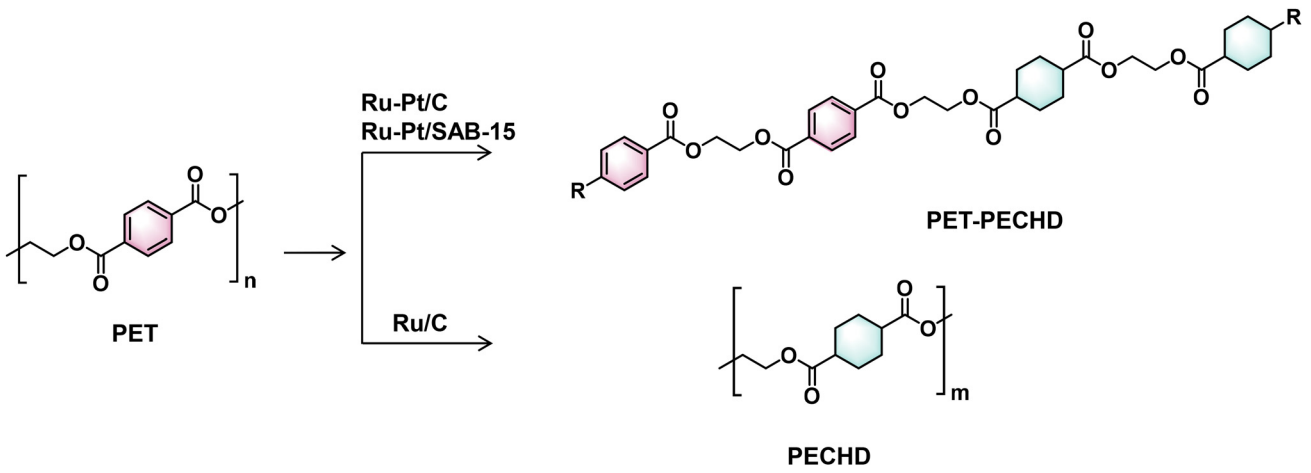

Scheme 2 Hydrogenation of PET to PET-PECHD and PECHD.

Table 1 Hydrogenation of PET over different catalysts to yield PET-PECHD and PECHD

Entry	Catalysts	Product	T (°C)	P_{H_2} (MPa)	t (h)	Yield (%)	Ref.
1	Ru–Pt/C	PECHD	50	6.89	1	100	25
2	Ru–Pt/SBA-15	PECHD	90	6.89	1.33	100	26
3	Ru/C	PET-PECHD	160	4	1	87	27

method used for catalyst preparation is crucial for generating RhO_x species, which enhance the adsorption of aromatic rings. Moreover, the synergistic effect of the Rh–Pt bimetallic catalyst, where Rh selectively hydrogenates aromatic rings while Pt facilitates H_2 spillover, contributes significantly to its high performance. After the hydrogenation of PET, PECHD was recovered to a very high extent using the compressed CO_2 anti-solvent technique. To address the significant drawback of using the environmentally hazardous solvent HFIP, the same research group proposed an on-water hydrogenation method for converting PET into PECHD using a Rh–Pt/SBA-15 catalyst. The catalyst was synthesized *via* chemical fluid deposition, employing supercritical CO_2 as the solvent. After optimizing the reaction conditions (90 °C, 6.89 MPa H_2 for 80 min), complete hydrogenation could be achieved. Unlike in HFIP solvent, water plays a crucial role in polarizing the aromatic rings of PET through proton donation, thereby establishing a connection between the catalyst surface and the aromatic rings of PET *via* hydrogen bonding at the aqueous interface between the catalyst and reactant. Furthermore, the synergistic effect of Rh–Pt enhances the hydrogenation performance: favorable adsorption of PET's aromatic rings on Pt(111) and efficient H_2 activation and spillover on the surface of Rh–Pt alloy nanoparticles make them more susceptible to selective hydrogenation by Rh. Additionally, the hydrophilicity of the SBA-15 support and the presence of surface –OH groups are critical for facilitating the on-water hydrogenation process. After the reaction, PECHD can be easily separated from the catalyst through simple centrifugation and drying.

Recently, the group of Ma proposed a partial hydrogenation strategy for converting PET into degradable PET-PECHD polyester.[27] This process involves partially hydrogenating aromatic rings (x) to aliphatic ones (y) using a Ru/C catalyst in dioxane solvent at 160 °C and 4 MPa H_2. The degree of hydrogenation can be precisely controlled by adjusting the reaction time. When the ratio of x/y exceeds 87/13, the molecular weight (M_w) remains stable due to minimal depolymerization. However, further hydrogenation leads to significant depolymerization, resulting in a blend of PET-PECHD and PECHD with lower M_w, and ultimately yielding a single-type PECHD polymer. Matrix-assisted laser desorption ionization time-of-flight mass spectrometry (MALDI-TOF MS) confirmed that depolymerization occurred *via* a hydrolysis process, as evidenced by the presence of hydroxyl or carboxyl terminal groups. Nevertheless, the underlying mechanism responsible for the exceptional hydrogenation performance of the Ru/C catalyst remains unclear.

3. Hydroconversion of PET for the production of 1,4-cyclohexanedicarboxylic acid (CHDA), dimethyl cyclohexane 1,4-dicarboxylate (DMCD) and bis(2-hydroxyethyl) cyclohexane-1,4-dicarboxylate (BHCD)

The depolymerization of PET through hydrolysis, methanolysis and glycolysis can produce aromatic monomers such as TPA,

DMT and BHET, respectively.[22] Conversely, when depolymerization is conducted under hydrogen in the presence of a metal-based catalyst, the aromatic units can be saturated, resulting in ring-saturated monomers like CHDA, DMCD and BHCD. These ring-saturated compounds are valuable intermediates for applications in polyester synthesis, pharmaceuticals, and coatings.[33–35] In addition, these ring-saturated compounds can also serve as the reagents for the production of CHDM, which is a key monomer for synthesizing advanced functional polyesters such as poly(ethylene terephthalate-1,4-cyclohexanedimethylene terephthalate) (PETG) and poly(1,4-cyclohexylene dimethylene terephthalate) (PCT).[24] In the hydrogenation of PET to ring-saturated monomers, the critical challenge lies in selectively saturating the aromatic rings while preserving the ester and carboxylic groups of the monomers. The performances of all related catalysts are summarized in Table 2.

3.1 Hydroconversion of PET for the production of CHDA

In the past decades, the production of CHDA has primarily focused on the ring hydrogenation of the PET hydrolyzed monomer TPA using a Pd/C catalyst (Scheme 3, Route I).[24] Under conditions of 250 °C and 12 MPa for 1 h, the yield of CHDA can reach up to 99%. To simplify the reaction pathway, Liu *et al.* demonstrated a one-pot hydrolysis–hydrogenation process for converting PET into CHDA (Scheme 3, Route II). Various carbon-supported metal-based catalysts, including Pd/C, Pt/C, Ru/C, Ni/C, Co/C, and Cu/C, were screened, with Pd/C showing the best performance, achieving 84.5% CHDA yield with 100% PET conversion at 200 °C and 3 MPa for 5 h.[36] The superior activity and selectivity of Pd/C for aromatic ring saturation are likely attributed to its lower oxophilicity compared to other metals tested, which preferentially adsorb the arene ring of TPA. The reaction route mainly involves hydrolysis and hydrogenation. In the presence of Pd/C, the conversion of PET is significantly faster than in its absence; this can be attributed to the hydrogenation of TPA to CHDA. CHDA exhibits higher solubility in water than TPA, leading to an increased acid concentration that catalyzes the hydrolysis of PET's ester groups. Additionally, the high acid site concentration of the Pd/C support may further accelerate the hydrolysis rate. Besides CHDA, several by-products, including 4-(hydroxymethyl)cyclohexanecarboxylic acid (HMCA), 4-methylcyclohexanecarboxylic acid (MHA), and cyclohexanecarboxylic acid (CCA), were also produced, with HMCA being the main side product. Time-dependent and control experiments with key intermediates revealed that both TPA and HMCA originated from BHET, which served as the key intermediate in this process. TPA is produced *via* the ester hydrolysis of BHET, while HMCA formation occurs through tandem hydrogenation, asymmetric ester hydrolysis, and hydrogenation of one ester group. Other side products, such as CCA and MHA, are generated *via* the asymmetric hydrogenation of TPA. However, the catalyst exhibited substantial deactivation after four cycles, likely attributed to the aggregation of metal species under the reductive hydrothermal conditions.

To eliminate the need for external H_2, Ma's group proposed an elegant tandem process combining the reforming of EG and hydrogenation for the one-pot conversion of PET into CHDA without the use of external H_2 (Scheme 3, Route III).[37] In this process, H_2 is generated from the reforming of EG with H_2O and consumed in the hydrogenation of the aromatic ring of TPA. A physical mixture of commercial Ru/C and Pd/C catalysts at a mass ratio of 3 : 1 proves effective at this transformation. Under conditions of 200 °C for 20 h, the yield of CHDA can reach up to 90%. In this system, Pd/C plays a critical role in the reforming reaction to generate hydrogen, while Ru/C catalyzes the hydrogenation of the aromatic ring. The addition of NaOH is crucial as it accelerates the reforming process and removes inhibitory species such as carboxylic acids and CO,

Table 2 Hydrogenation of PET over different catalysts to yield CHDA, DMCD and BHCD

Entry	Substrate	Catalysts	Products	Solvent	T (°C)	P_{H_2} (MPa)	t (h)	Yield (%)	Ref.
1	TPA	Pd/C	CHDA	H_2O	250	12	1	99	24
2	PET	Pd/C	CHDA	H_2O	200	3	5	84.5	36
3	PET	NaOH + Pd/C + Ru/C	CHDA	H_2O	200	—	20	90	37
4	DMT	Pd/HT_c–Al_2O_3	DMCD	—	225	6	—	95	38
5	DMT	RuPd/HT_c–Al_2O_3	DMCD	Ethyl acetate	180	8	6	95.7	39
6	DMT	SiO_2@Ru@NC	DMCD	Methanol	90	2	2	92.2	40
7	DMT	Ru/Al-SBA-15	DMCD	H_2O	100	4.14	0.5	93.4	41
8	DMT	RuPd/Al_2O_3	DMCD	Ethyl acetate	180	8	6	85.1	42
9	DMT	Ru/Ni/Ni(Al)O_x	DMCD	Isopropanol	90	5	5	92.5	43
10	DMT	Ru–Ni/CNT	DMCD	Ethyl acetate	150	6	1	76	44
11	DMT	Ni/NiAlO_x/Al_2O_3	DMCD	Isopropanol	90	6	4	93.3	45
12	DMT	K–Ni/SiO_2	DMCD	Isopropanol	90	5	4	91.2	46
13	DMT	NiLa-40 wt%	DMCD	Dioxane	140	5	5	90.4	47
14	PET	CuFeCr	DMCD	Dioxane	240	3 (CO_2 : H_2 = 1 : 1)	48	28.6	48
15	PET	Pd–Ni/CeO_2	DMCD	Methanol	180	6	10	86.5	51
16	PET	CeO_2/Ni	DMCD	Methanol	170	4	24	80	52
17	PET	Ru/MnO_2	DMCD	Methanol	140	4	8	84.3	49
18	PET	Ru/UiO-66_{def}-SO_3H	DMCD	Methanol	170	3	6	97.7	50
19	BHET	Pd/C	BHCD	—	155	3.5	7	~95	53
20	BHET	Ru/*m*-HZSM-5	BHCD	Cyclohexane	120	3	2	91.3	54

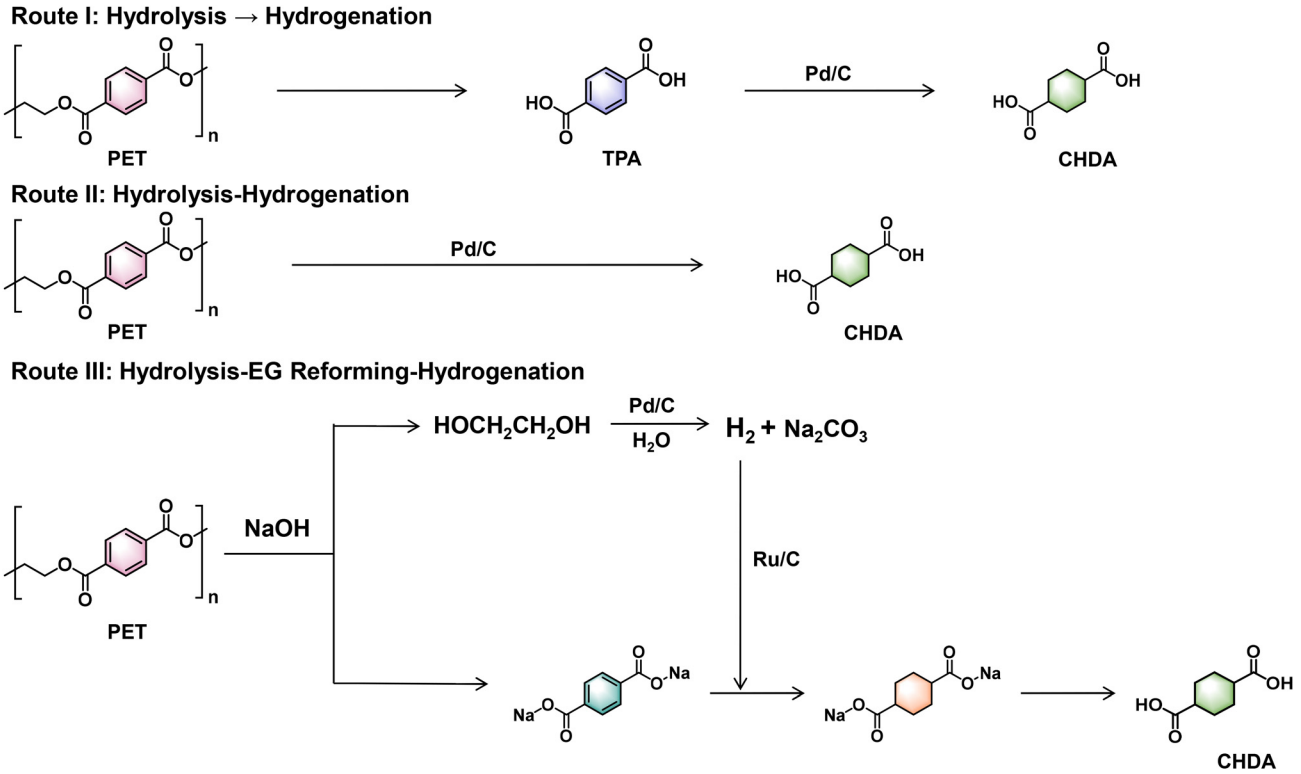

Scheme 3 Routes for the conversion of PET into CHDA.

thereby maintaining a favorable environment for subsequent hydrogenation over Ru/C. In addition, NaOH catalyzed the initial hydrolysis depolymerization reaction of PET to TPA and EG. This catalytic combination can be applied to the conversion of post-consumer transparent PET bottles, yielding 75% CHDA with 96% purity at 180 °C for 25 h. However, it is less effective for fibers from pillow fillers and colored bottles, likely due to the influence of impurities. Additionally, this catalytic system suffers from severe deactivation, with the CHDA yield declining from ~85% to ~15%, and eventually to 0%; this is attributed to the sintering of metal nanoparticles. Additional improvements in catalyst stability and the development of non-noble metal catalysts are necessary.

3.2 Hydroconversion of PET for the production of DMCD

In previous studies, the conversion of PET to DMCD was primarily achieved *via* methanolysis to DMT followed by the hydrogenation of DMT to DMCD (Scheme 4, Route I). In the hydrogenation of DMT to DMCD, the critical challenge lies in selectively saturating the aromatic rings while preserving the ester groups. Various catalysts have been developed for this purpose, including Pd/HT_c–Al_2O_3,[38] RuPd/HT_c–Al_2O_3,[39] SiO_2@Ru@NC,[40] Ru/Al-SBA-15,[41] RuPd/Al_2O_3,[42] Ru/Ni/Ni(Al)O_x,[43] Ru–Ni/CNT,[44] Ni/$NiAlO_x$/Al_2O_3,[45] potassium-modified Ni/SiO_2,[46] and NiLa-40 wt%.[47] High metal dispersion, strong hydrogen adsorption capacity, and efficient hydrogen release are key factors contributing to achieving high activity and high-yielding DMCD production. Additionally, basic modifiers or supports play a crucial role in enhancing the performance of Ni-based catalysts by increasing the density of metallic nickel sites and reducing acid sites that inhibit the hydrogenolysis of esters. Using these advanced catalysts, the yield of DMCD can reach up to 95.7% under mild reaction conditions (Table 2).

To reduce the number of reaction and separation steps and enhance the economic feasibility of PET upcycling, a tandem reaction strategy that integrates methanolysis and aromatic ring hydrogenation in a one-pot process was recently demonstrated (Scheme 4, Route II). Ma *et al.* pioneered an innovative approach by coupling CO_2 hydrogenation to methanol with the methanolysis–hydrogenation of PET to produce DMCD over a CuFeCr catalyst in a one-pot process[48] (Fig. 1a). However, the yield of DMCD was relatively low (28.6%), likely due to the limited aromatic ring hydrogenation ability of Cu-based catalysts.

To further improve the yield of DMCD from PET, Wang *et al.* developed a Pd-Ni/CeO_2 catalyst for the tandem methanolysis–hydrogenation conversion of PET in methanol solvent with hydrogen, achieving a remarkable yield of 86.5% DMCD under conditions of 180 °C, 6 MPa H_2 for 10 h (Scheme 4, Route III).[51] The catalyst can convert dyed polyester fabric, beverage bottles and PET film into DMCD with yields of 86.0–88.3%. In addition, the catalyst can be reused after being regenerated by re-reduction. In this bimetallic catalyst, Ni species serve as the primary active sites, while the addition of Pd significantly improves the selectivity toward DMCD.

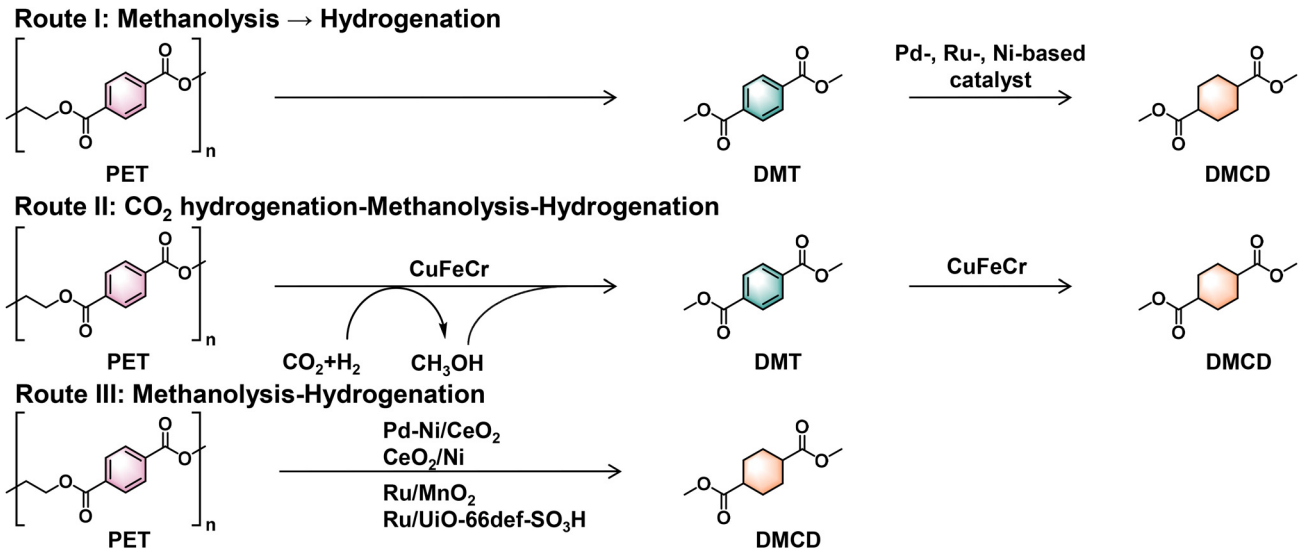

Scheme 4 Routes for the conversion of PET into DMCD.

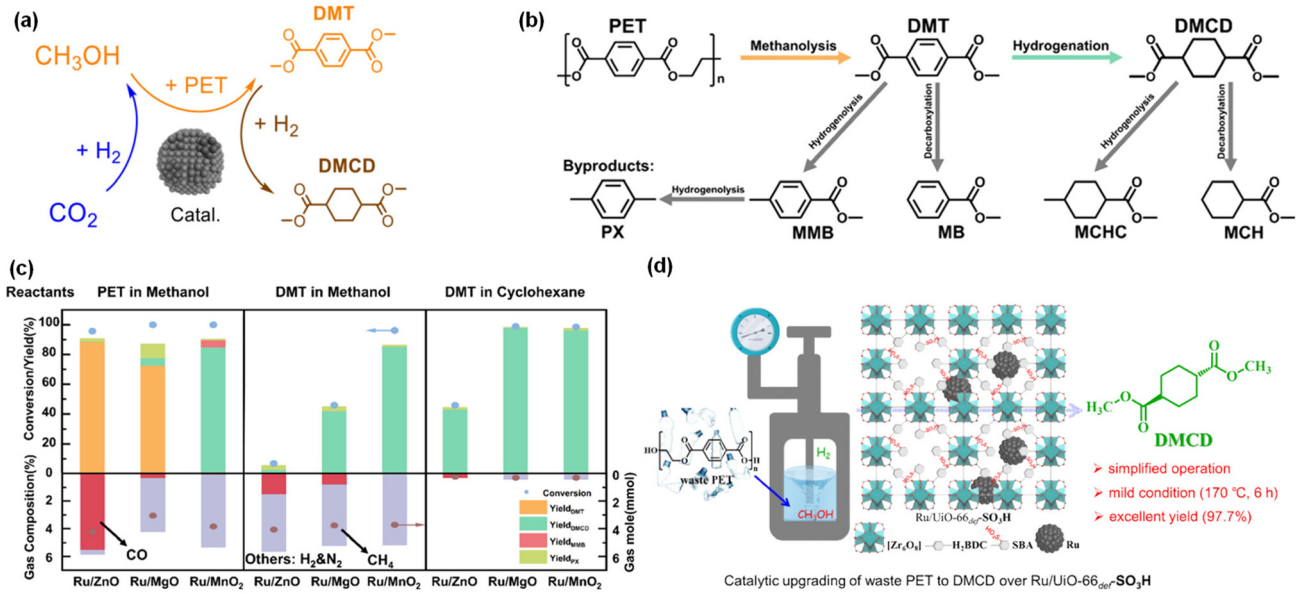

Fig. 1 (a) The one-pot catalytic conversion of CO_2 and PET into DMCD over the CuFeCr catalyst. Reproduced with permission.[48] Copyright 2022, Wiley-VCH. (b) Reaction pathway for the tandem methanolysis–hydrogenation of PET to DMCD. Reproduced with permission.[49] Copyright 2025, American Chemical Society. (c) Comparison of the liquid and gas phase products of Ru/ZnO, Ru/MgO, and Ru/MnO_2. Reproduced with permission.[49] Copyright 2025, American Chemical Society. (d) The tandem methanolysis–hydrogenation of PET to DMCD over the Ru/UiO-66_{def}-SO_3H catalyst. Reproduced with permission.[50] Copyright 2025, Elsevier.

Characterization studies and temperature-programmed desorption coupled with mass spectrometry (TPD-MS) experiments using ethyl acetate revealed that the incorporation of Pd enhanced the metallic character of Ni species, weakening their ability to adsorb and activate C–O bonds, thereby inhibiting the hydrogenolysis of ester bonds. This is further evidenced by the higher DMCD yield (78.8%) achieved over a 5 wt% Ni/CeO_2 catalyst reduced at 500 °C compared to 66.2% when reduced at 400 °C. However, Li *et al.* reported that a 4 wt% Ni/CeO_2 catalyst exhibited a relatively low DMCD yield (8.1%) in the tandem methanolysis–hydrogenation of PET.[52] The differing performances of Ni/CeO_2 catalysts with comparable Ni loadings can be attributed to variations in catalyst preparation methods; Wang's group employed the impregnation method, whereas Li's group used the coprecipitation method. On the other hand, Li's group discovered that an inverse CeO_2/Ni catalyst could effectively convert PET into DMCD with a yield of 80%.[52] However, a low feed ratio (PET : catalyst = 1 : 1–1.25 : 1)

and long reaction time (10–24 h) are needed to achieve high yields of DMCD over both Pd–Ni/CeO_2 and inverse CeO_2/Ni catalysts, thereby rendering the process less efficient.

To further enhance the productivity of DMCD, Cheng *et al.* developed a Ru/MnO_2 catalyst for the one-pot tandem methanolysis–hydrogenation conversion of PET into DMCD.[49] This catalyst achieved an impressive yield of 84.3% DMCD under conditions of 140 °C, 4 MPa H_2 for 8 h with a feed ratio of 5 : 1. Moreover, this catalyst is applicable for converting waste PET materials, including beverage bottles, clothing fabrics, scarves, and packaging films, into DMCD with yields ranging from 84% to 85% after 6–8 h. The catalyst exhibited excellent stability, with the DMCD yield decreasing only slightly from 80% to 77% after five consecutive reaction cycles. Time-dependent experiments revealed that the hydrogenation of aromatic rings predominantly occurred after depolymerization, indicating that the methanolysis of PET to DMT was the rate-determining step (Fig. 1b). A variety of basic, amphoteric, and acidic metal oxides were investigated, with basic oxides proving effective at the depolymerization of PET to DMT. Although Ru-based catalysts supported on basic oxides (Ru/MnO_2, Ru/MgO, Ru/ZnO) can effectively hydrogenate DMT to DMCD, only Ru/MnO_2 enables the tandem methanolysis–hydrogenation of PET to DMCD. The generation of CO during the tandem process represents a toxic gas that inhibits the catalyst's ability to hydrogenate aromatic rings (Fig. 1c). However, compared to Ru/MgO and Ru/ZnO catalysts, Ru/MnO_2 exhibits superior low-temperature CO methanation activity, enabling the removal of toxic CO in the form of methane, thereby facilitating aromatic ring hydrogenation. This phenomenon can be attributed to the electronic metal–support interaction, which enriches the electron density on the Ru surface. This not only activates adsorbed CO and enhances low-temperature methanation activity but also strengthens the adsorption of the electron-deficient aromatic ring of the DMT molecule, promoting the reduction of aromatic rings. In addition to the basic MnO_2 support, acidic UiO-66_{def}-SO_3H also serves as an excellent support for this tandem process[50] (Fig. 1d). The resulting Ru/UiO-66_{def}-SO_3H catalyst features mesopores, an enlarged surface area, enhanced acidity, and highly dispersed Ru nanoparticles, exhibiting outstanding catalytic performance in converting PET into DMCD with a yield of 97.7% at 170 °C, 3 MPa H_2 for 6 h under a high feed ratio of 20 : 1. This catalyst is also capable of converting PET wastes including beverage bottles, textile fibers, and packaging film into DMCD with yields ranging from 92.8% to 95.4%. Mechanistic studies revealed that acidic sites, including Zr–O nodes, Zr–OH, and –SO_3H groups, played a critical role in the methanolysis depolymerization of PET to DMT, while metallic Ru sites were responsible for the hydrogenation of aromatic rings. Notably, the catalyst can be recycled for five consecutive runs without experiencing deactivation.

3.3 Hydroconversion of PET for the production of BHCD

The reductive depolymerization of PET to BHCD was rarely reported in recent studies. The production of BHCD primarily involves a two-step process consisting of glycolysis followed by hydrogenation (Scheme 5, Route I). To date, there are no reports on the one-pot tandem glycolysis–hydrogenation conversion of PET into BHCD. In 2015, Zhang *et al.* demonstrated the hydrogenation of BHET, obtained *via* glycolysis of PET, using a Pd/C catalyst under solvent-free conditions.[53] After optimizing the reaction conditions, the conversion of BHET and the yield of BHCD reached 95%, at 155 °C, 7 MPa H_2 for 3 h. To achieve high yields of BHCD under mild reaction conditions, Hou *et al.* developed a mesoporous Ru/*m*-HZSM-5 catalyst for the hydrogenation of BHET to BHCD.[54] The conversion of BHET and the selectivity of BHCD over this catalyst reached 95.5% and 95.6%, respectively, at 120 °C, 3 MPa H_2 for 2 h. It was found that metallic Ru served as the active site for aromatic ring hydrogenation. Compared to microporous Ru/HZSM-5, the Ru/*m*-HZSM-5 catalyst exhibits mesopores, an enlarged specific surface area, and highly dispersed Ru nanoparticles, which enhance the hydrogenation of the benzene rings in BHET. This catalyst can be recycled at least five times without significant loss of activity or selectivity. Although high yields of BHCD can be achieved through the hydrogenation of BHET, the development of catalysts for the one-pot tandem glycolysis–hydrogenation process remains essential for process intensification.

4 Hydroconversion of PET for the production of CHDM

CHDM is a critical monomer for the synthesis of high-value polyesters such as PETG, PCT, and poly(1,4-cyclohexylenedimethyleneterephthalate glycol) (PCTG). The incorporation of CHDM units imparts these polymers with exceptional properties compared to PET, including enhanced biodegradability, elevated glass transition temperatures, improved thermal resistance, and superior mechanical strength.[31,32] Currently,

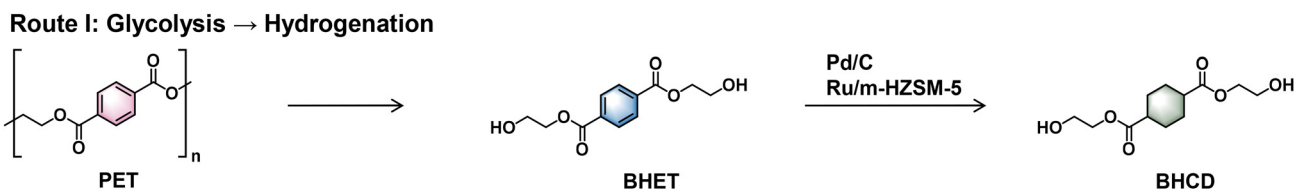

Scheme 5 The route for the conversion of PET into BHCD.

CHDM is predominantly produced from petroleum-derived *para*-xylene (PX) through oxidative and hydrogenation processes, using DMT as an intermediate under stringent reaction conditions (Scheme 6, Route I).[55] However, utilizing PET waste can provide a sustainable pathway for the production of this valuable monomer, which also represents a promising approach for upcycling PET plastic waste. Typically, the production of CHDM from PET waste involves four distinct strategies: (1) three-step methanolysis/glycolysis to DMT/BHET, followed by hydrogenation to DMCD/BHCD and hydrogenolysis to CHDM (Scheme 6, Route II); (2) two-step methanolysis/hydrolysis–hydrogenation to DMCD/CHDA, followed by hydrogenolysis to CHDM (Scheme 6, Route III); (3) two-step methanolysis/hydrolysis to DMT/TPA, followed by hydrogenation–hydrogenolysis to CHDM (Scheme 6, Route IV); (4) one-pot hydrogenation–hydrogenolysis of PET directly to CHDM (Scheme 6, Route V). The primary challenge in the production of CHDM from PET and PET-derived monomers lies in achieving selective hydrogenolysis of the ester group while maintaining the integrity of the hydroxyl group. In this respect, Cu-based catalysts are often used in this strategy to achieve high yields of CHDM. Table 3 summarize the performances of the catalysts that were used in different routes.

4.1 Three-step methanolysis/glycolysis, hydrogenation and hydrogenolysis to yield CHDM

In recent decades, extensive research has been conducted on the three-step conversion of PET into CHDM *via* methanolysis, hydrogenation, and hydrogenolysis (Scheme 6, Route II). PET can be effectively depolymerized with methanol at temperatures above 200 °C, yielding high amounts of DMT and EG.[47] Regarding the hydrogenation of DMT to DMCD, various metallic catalysts, including Pd-, Ru-, and Ni-based catalysts, have been investigated.[38–47] This topic is elaborated upon in Section 3. For the hydrogenolysis of DMCD to CHDM, Cu-based catalysts are predominantly utilized. Industrially, a CuCr catalyst is employed under hydrogen pressures ranging from 30 to 48 MPa.[56] However, Cr poses significant environmental toxicity concerns.[47] Consequently, the development of environmentally friendly and highly active Cu-based catalysts has garnered increasing attention. Several novel Cu-based catalysts, such as Cu/SiO_2,[57] CuMgAl,[58] Cu/MgO,[59] $Cu/Mg_3Sc_2O_6$,[60] and $CuFeAl_{0.5}$,[47] have been successfully developed, achieving CHDM yields up to 99.8%. The synergistic catalytic effect between active metallic copper species (Cu^0) and Lewis acid/basic sites (Cu^+ or support), which facilitate hydrogen dis-

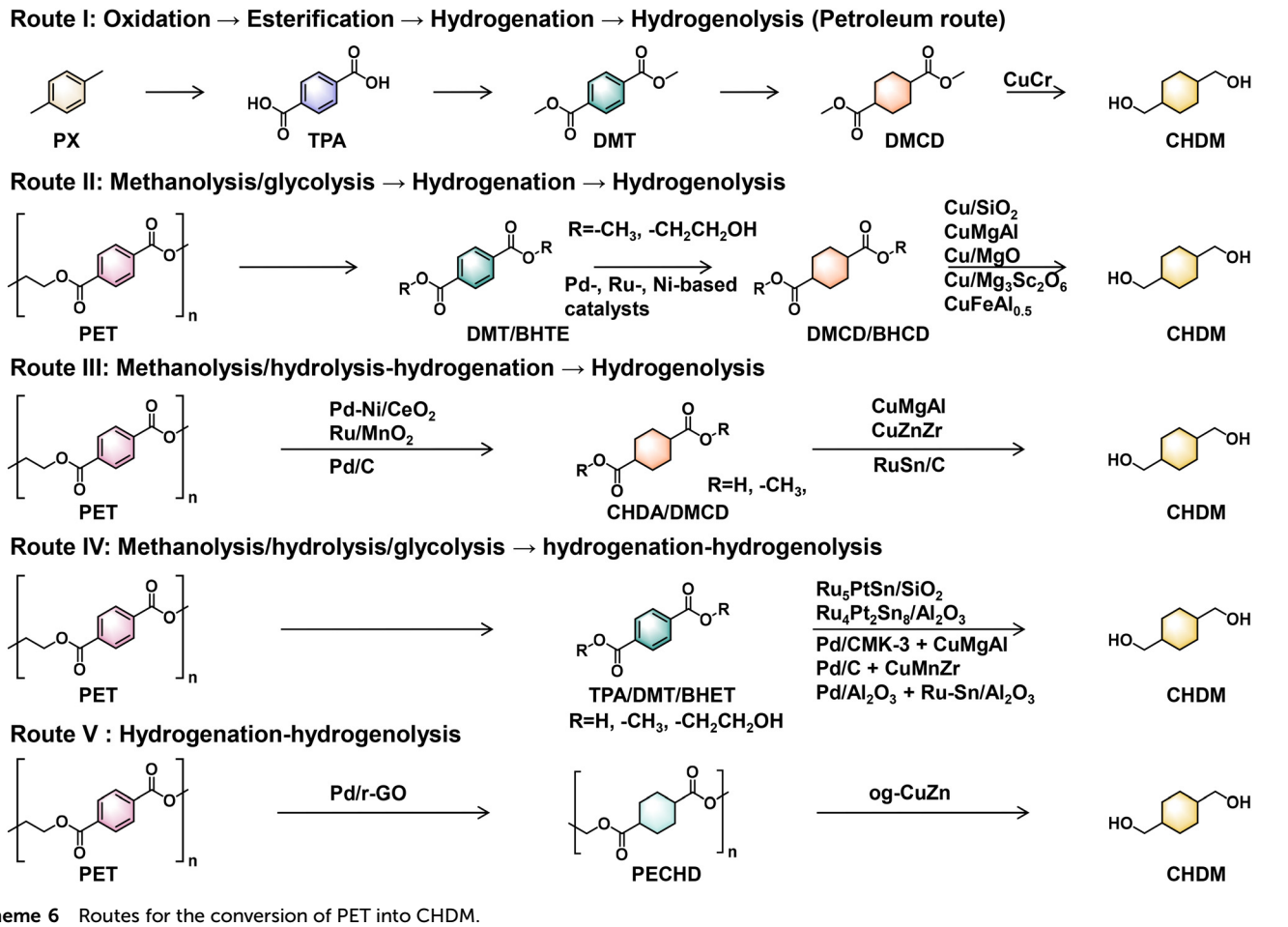

Scheme 6 Routes for the conversion of PET into CHDM.

Table 3 Hydrogenation of PET over different catalysts to yield CHDM

Entry	Substrate	Method	Catalysts	Products	Solvent	T (°C)	P_{H_2} (MPa)	t (h)	Yield (%)	Ref.
1	PET	Methanolysis	—	DMT	Methanol	250	—	2	100	47
		Hydrogenation	NiLa-40 wt%	DMCD	Dioxane	150	5	5	90.4	
		Hydrogenation	CuFeAl	CHDM	Dioxane	250	5	2	99.8	
2	PET	Glycolysis	—	BHET	EG	—	—	—	—	53
		Hydrogenation	Pd/C	BHCD	—	155	3.5	7	~95	
		Hydrogenation	Cu–Zn/Al_2O_3	CHDM	—	270	8.5	6	78	
3	PET	Methanolysis–hydrogenation	Pd–Ni/CeO_2	DMCD	Methanol	180	6	10	86.5	51
		Hydrogenation	CuMgAl	CHDM	Methanol	250	5	4	83.8	
4	PET	Methanolysis–hydrogenation	Ru/MnO_2	DMCD	Methanol + dioxane	140	4	8	82	49
		Hydrogenation	CuZnZr	CHDM	Methanol + dioxane	250	3	4	95.6	
5	PET	Hydrolysis–hydrogenation	Pd/C	CHDA	H_2O	200	3	5	84.5	36
		Hydrogenation	RuSn/C	CHDM	H_2O	250	5	6	80.1	
6	DMT	Hydrogenation–hydrogenolysis	Ru_5PtSn/SiO_2	CHDM	Ethanol	100	2	24	45.5	55
7	DMT	Hydrogenation–hydrogenolysis	$Ru_4Pt_2Sn_8/Al_2O_3$	CHDM	Ethanol	180	6	2	75.1	62
						260	8.5	8		
8	DMT	Hydrogenation–hydrogenolysis	Pd/CMK-3 + CuMgAl	CHDM	Dioxane	250	5	3	82.3	63
9	PET	Methanolysis	—	DMT	Methanol	220	0.1	6	—	64
						250	5	WHSV = 2.5 h^{-1}		
		Hydrogenation–hydrogenolysis	Pd/C + CuMnZr	CHDM	Dioxane	250	5	WHSV = 0.8 h^{-1}	85.7	
10	TPA	Hydrogenation–hydrogenolysis	Pd/Al_2O_3 + Ru–Sn/Al_2O_3	CHDM	—	180	4	1.5	72.2	65
						230	5	5		
11	TPA	Hydrogenation–hydrogenolysis	Pd–Ce/Al_2O_3 + Ru–Sn/Al_2O_3	CHDM	—	180	5	1.5	85.5	66
						230	8	5		
12	BHET	Hydrogenation–hydrogenolysis	RuPtSn/Al_2O_3	CHDM	—	170	5	2	87.1	67
						260	5	6		
13	PET	Hydrogenation–hydrogenolysis	Pd/r-GO + og-CuZn	CHDM	Dioxane	120	4	6	95	28
						200	8			

sociation and carbonyl group activation, plays a crucial role in enhancing the hydrogenolysis reaction. Recently, Li *et al.* demonstrated this process starting with PET methanolysis at 250 °C for 2 h, achieving nearly 100% DMT yield.[47] The resulting DMT was diluted with 1,4-dioxane and subsequently hydrogenated to DMCD over a NiLa-40 wt% catalyst under conditions of 150 °C, 5 MPa H_2 for 5 h, achieving a DMCD yield of 90.4%. Following catalyst filtration, DMCD was further hydrogenolyzed to CHDM using a CuFeAl catalyst at 250 °C, 5 MPa H_2 for 2 h, resulting in an overall CHDM yield of 90.2%.

The glycolysis of PET to BHET, the hydrogenation of BHET to BHCD, and the subsequent hydrogenolysis of BHCD to CHDM represent another promising pathway for the conversion of PET into CHDM. In 2015, Zhang *et al.* developed this process starting with PET glycolysis.[53] The BHET product obtained from PET glycolysis was extracted and subsequently hydrogenated to BHCD using a 10% Pd/C catalyst under solvent-free conditions at 155 °C and 7 MPa of hydrogen pressure. Subsequently, BHCD was hydrogenolyzed to CHDM over a Cu–Zn/Al_2O_3 catalyst, achieving 87% yield. Characterization studies revealed that Cu^0/Cu^+ species served as the active sites for the hydrogenolysis of BHCD to CHDM. In addition to the Cu–Zn/Al_2O_3 catalyst, Hou *et al.* developed a Cu/$MgAl_2O_4$ catalyst by calcining and reducing a CuMgAl-LDH precursor.[61] The resulting catalyst exhibited a high surface area, strong metal–support interactions, and abundant basic sites, enabling a CHDM yield of 98% at 240 °C and 4 MPa H_2. Furthermore, the catalyst maintained its activity for at least 80 h of continuous operation. The basic sites of the Cu/$MgAl_2O_4$ catalyst enhanced the adsorption and activation of the C=O bond, thereby improving the catalytic activity.

4.2 Two-step methanolysis/hydrolysis–hydrogenation and hydrogenolysis to yield CHDM

The two-step methanolysis/hydrolysis–hydrogenation of PET to DMCD/CHDA, followed by hydrogenolysis to CHDM, provides an economically viable pathway for CHDM production while eliminating the need for a separate methanolysis/hydrolysis step (Scheme 6, Route III). Techno-economic analysis (TEA) indicated that this two-step process reduced capital investment by 22% compared to the conventional three-step route (PET → DMT → DMCD → CHDM).[49]

For the tandem methanolysis–hydrogenation conversion of PET into DMCD, the primary challenge lies in developing highly active hydrogenation catalysts capable of achieving aromatic ring saturation while preserving ester bonds. Furthermore, the catalyst must exhibit tolerance to CO poisoning, as outlined in Section 3. Wang *et al.* demonstrated this

strategy using a Pd–Ni/CeO_2 catalyst for the tandem methanolysis–hydrogenation of PET to DMCD, achieving a yield of 86.5% at 180 °C, 6 MPa H_2 for 10 h, and a CuMgAl catalyst for the subsequent hydrogenolysis of DMCD to CHDM, achieving a yield of 83.8% under conditions of 250 °C, 5 MPa H_2 for 4 h.[51] The isolated CHDM product exhibited a purity of 72% with a *trans*/*cis* ratio of 3.32. Both processes utilize methanol as the solvent, enabling process integration through simple filtration. Techno-economic analysis (TEA) revealed that the production cost of CHDM using this method was approximately 22 500 CNY per t, significantly lower than the market price of 31 000 CNY per t. To further enhance productivity under mild reaction conditions, Cheng *et al.* developed a Ru/MnO_2 catalyst for the one-pot tandem methanolysis–hydrogenation conversion of PET into DMCD and a CuZnZr catalyst for the subsequent hydrogenolysis of DMCD to CHDM.[49] The yield of DMCD reached 84.3% under conditions of 140 °C, 4 MPa H_2 for 8 h, while the yield of CHDM achieved 78% with a purity of >98% under conditions of 250 °C, 3 MPa H_2 for 4 h. The superior performance of the CuZnZr catalyst can be attributed to its uniform Cu dispersion, which significantly increases the density of active sites. The catalyst can be recycled three times without deactivation. More importantly, the Ru/MnO_2 and CuZnZr catalyst system can successfully transform 1 g PET waste into 0.57 g CHDM with a purity of >98%. The overall yield of CHDM could reach 78%.

In addition to the two-step methanolysis–hydrogenation and hydrogenolysis strategy, Liu *et al.* demonstrated a two-step hydrolysis–hydrogenation and hydrogenolysis process for converting PET into CHDM.[36] Pd/C and RuSn/C catalysts were developed for the hydrolysis–hydrogenation of PET to the CHDA intermediate and the subsequent reduction of CHDA to CHDM, achieving a yield of 86.4% under conditions of 250 °C, 5 MPa H_2 for 10 h. Furthermore, this approach yielded 76.9% CHDM from real post-consumer PET bottles. Water was used as the solvent in both stages of the process. Characterization studies revealed that the active site of the RuSn/C catalyst responsible for reducing COOH groups into CH_2OH was the Ru_3Sn_7 alloy. However, the RuSn/C catalyst exhibited significant deactivation during recycling, which could be attributed to the leaching of Ru and Sn components.

4.3 Two-step methanolysis/hydrolysis/glycolysis and hydrogenation–hydrogenolysis to yield CHDM

The methanolysis/hydrolysis/glycolysis process can yield DMT/TPA/BHET monomers, which can subsequently be converted into CHDM *via* a tandem hydrogenation–hydrogenolysis process (Scheme 6, Route IV). Catalysts employed in this tandem process include trimetallic catalysts as well as mixtures of Pd-based[55,62] and Cu-based catalysts.[63,64]

Hungria *et al.* first developed a Ru_5PtSn/SiO_2 trimetallic catalyst for the one-pot hydrogenation–hydrogenolysis of DMT to CHDM under mild reaction conditions (100 °C, 2 MPa H_2 for 24 h).[55] However, the conversion of DMT (63.9%) and the selectivity of CHDM (71.2%) were relatively low, falling far short of industrial requirements. Subsequently, an Al_2O_3-supported trimetallic $Ru_4Pt_2Sn_8/Al_2O_3$ catalyst was further developed for the one-pot conversion of DMT into CHDM through two consecutive reaction stages at different temperatures (180 °C and 260 °C).[62] The lower temperature promotes the aromatic ring hydrogenation of DMT to DMCD, while the higher temperature facilitates the hydrogenolysis reaction. Using this approach, the conversion of DMT and the yield of CHDM can reach 98.2% and 75.1%, respectively. Characterization studies revealed that two distinct active sites were separately loaded onto the support: Ru particles interacting with Pt (RuPt sites) and Ru particles solely embedded in SnO_2 (RuSn sites). The RuPt sites are responsible for the aromatic ring hydrogenation of DMT to yield DMCD, while the RuSn sites catalyze the hydrogenolysis of the ester group to alcohol products (Fig. 2a). However, the yield of CHDM remains relatively low, and the required hydrogen pressure is quite high (8.5 MPa).

To further enhance the yield of CHDM at a low hydrogen pressure, Li *et al.* reported a mixed Pd/CMK-3 + CuMgAl catalyst system for the one-pot conversion of DMT into CHDM.[63] This catalyst system achieved 82% yield of CHDM under reaction conditions of 250 °C, 5 MPa H_2 for 3 h. Mechanistic studies indicated that the Pd/CMK-3 catalyst was responsible for the hydrogenation of DMT to DMCD, while the CuMgAl catalyst was effective at the subsequent hydrogenolysis of the ester group to yield the alcohol (Fig. 2b). The optimal mass ratio (0.5) of Pd/CMK-3 and CuMgAl catalysts is critical for achieving high yields of CHDM. A higher amount of Pd/CMK-3 leads to a high yield of cyclohexanemethanol (CHM), whereas a higher amount of CuMgAl catalyst affords high yields of 4-methyl-1-cyclohexanemethanol (MCHM) and 1,4-dimethylcyclohexane (DMCH). However, the catalyst system exhibited instability after four cycles, with the yield of CHDM gradually declining from 82% to 43%. This can be attributed to Pd leaching during the reaction. In addition to the Pd/CMK-3 + CuMgAl catalyst system, the mixture of Pd/C and CuMnZr catalysts was also effective at the one-pot hydrogenation–hydrogenolysis of PET to CHDM, achieving a yield of 75.7% at 230 °C, 4 MPa H_2 for 8 h. Kinetic studies revealed that the hydrogenolysis of DMT to methyl 4-methyl benzoate (MMB) was the critical step that suppressed the formation of CHDM, likely due to the high activity of Cu-based catalysts for ester bond cleavage at elevated reaction temperatures. To further improve the yield of target CHDM, Wang *et al.* proposed a dual-temperature strategy (200 °C for 5 h followed by 230 °C for 6 h) for the conversion of DMT into CHDM, increasing the yield of CHDM to 92.6%.[64] It was found that Pd/C played a role in the hydrogenation of DMT to DMCD, while CuMnZr catalyzed the reduction of the ester group of DMCD to CHDM, consistent with the Pd/CMK-3 + CuMgAl system (Fig. 2c). Based on this, the authors proposed a controlled sequential hydrogenation strategy using a fixed-bed reactor with two catalyst bed layers (upper: Pd/C and lower: CuMnZr). More interestingly, the authors proposed an integrated process combining PET methanolysis and subsequent one-pot hydrogenation–hydrogenolysis for the conversion of PET into CHDM, achieving a yield of 85.7%. With this

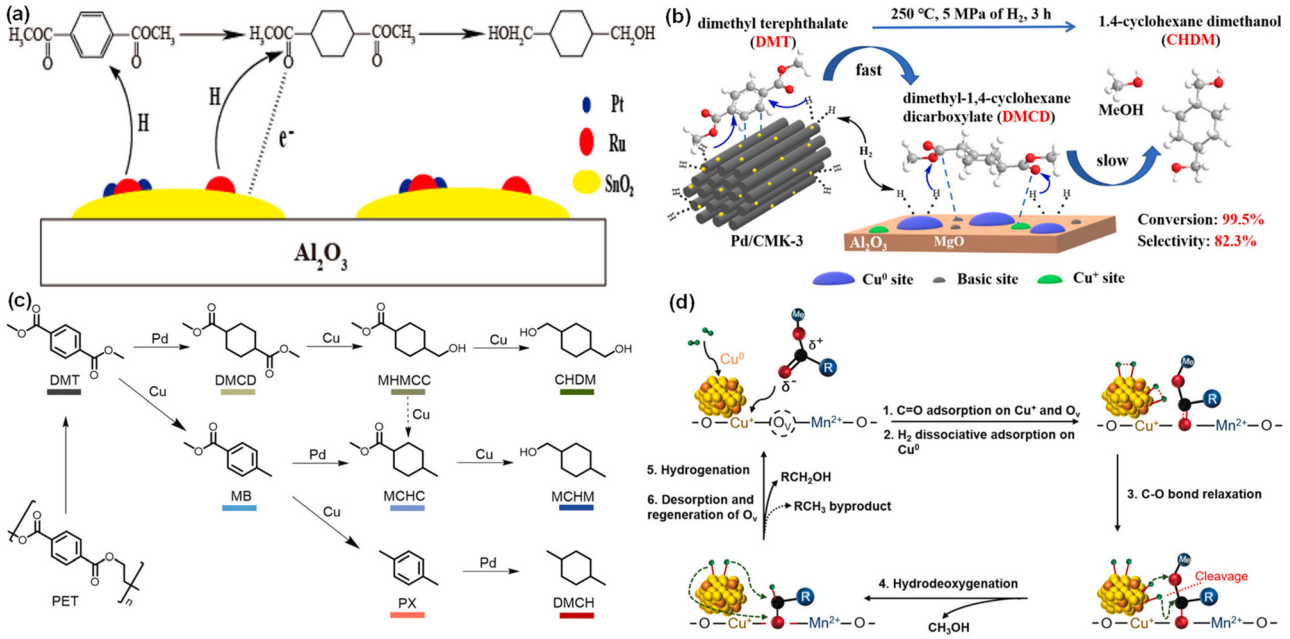

Fig. 2 (a) The proposed metal active sites of the RuPtSn/Al_2O_3 catalyst for the hydrogenation–hydrogenolysis of DMT to CHDM. Reproduced with permission.[62] Copyright 2014, American Chemical Society. (b) The proposed mechanism for the conversion of DMT into CHDM over physically-mixed Pd/CMK-3 and CuMgAl catalysts. Reproduced with permission.[63] Copyright 2022, Elsevier. (c) The reaction pathway for the conversion of DMT into CHDM over physically-mixed Pd/C and CuMnZr catalysts. Reproduced with permission.[64] Copyright 2025, Elsevier. (d) The oxygen vacancy-assisted mechanism of ester group hydrogenolysis over the CuMnZr catalyst. Reproduced with permission.[64] Copyright 2025, Elsevier.

integrated process, no additional 1,4-dioxane solvent is required. The yield of CHDM remained stable during 300 h of continuous operation. TEA indicated that the production cost of CHDM from this system was estimated to be 22 450 CNY per t, representing a 27.4% reduction compared to the current market price of 31 000 CNY per t. The high performance of the CuMnZr catalyst for the reduction of the ester group of DMCD to CHDM can be attributed to the formation of a Cu–O–Mn interface, increased Cu dispersion, and an optimal Cu^+/Cu^0 ratio (Fig. 2d). Cu^+ serves as the site for the absorption of the ester C=O bond. Furthermore, the formation of the Cu–O–Mn interface introduces a large number of oxygen vacancies adjacent to Cu^+, allowing the anchoring of the C=O group. Cu^0 activates hydrogen to form active H, breaking down the acyl C–O bond of the ester group and releasing methanol. Subsequently, CHDM is produced *via* the hydrogenation of the C=O group and subsequent desorption. Due to the decreased acid site density caused by Mn doping, the CuMnZr catalyst exhibits high selectivity toward alcohol products by effectively suppressing the undesired hydrogenolysis pathway, which is typically catalyzed by acid sites.

In addition to DMT, TPA and BHET can serve as intermediates for the production of CHDM *via* tandem hydrogenation–hydrogenolysis. In 2023, Zhang *et al.* developed a Pd/Al_2O_3 + Ru–Sn/Al_2O_3 mixed catalytic system for the one-pot tandem hydrogenation–hydrogenolysis of TPA to CHDM.[65] The process consisted of two stages conducted at different temperatures (180 °C, 4 MPa H_2 for 1.5 h followed by 230 °C, 8 MPa H_2 for 5 h). The Pd/Al_2O_3 catalyst facilitated aromatic ring hydrogenation at low temperature, while the Ru–Sn/Al_2O_3 catalyst was responsible for the hydrogenolysis of ester bonds to alcohol groups. With an optimized Sn/Ru ratio of 0.5, the yield of CHDM reached 72.2%. To further enhance the CHDM yield, 2 wt% Ce was incorporated into the Pd/Al_2O_3 catalyst to form a Pd–Ce/Al_2O_3 + Ru–Sn/Al_2O_3 composite catalyst system.[66] The addition of Ce improved metal dispersion and introduced oxygen vacancies, thereby enhancing hydrogen activation and C=O bond activation. Consequently, under identical reaction conditions, the CHDM yield increased from 72.2% to 85.5%. In 2016, Zhang *et al.* developed a trimetallic RuPtSn/Al_2O_3 catalyst for the one-pot conversion of BHET into CHDM.[67] This catalyst featured multiple active sites capable of catalyzing the hydrogenation of phenyl and carbonyl groups. As a result, a CHDM yield of 87.1% was achieved under dual-temperature stages (170 °C for 2 h followed by 260 °C for 6 h).

4.4 One-pot hydrogenation–hydrogenolysis for the production of CHDM

The one-pot conversion of PET into CHDM represents a straightforward and efficient approach, enabling process intensification while eliminating additional complex and energy-intensive purification steps. Recently, Cao's group developed a dual-catalyst system combining palladium on reduced graphene oxide (Pd/r-GO) and oxalate-gel-derived copper–zinc oxide (og-CuZn) catalysts for the one-pot hydrogenation–hydrogenolysis process to convert PET into CHDM (Scheme 6, Route V).[28] Initially, they conducted the entire reaction at 200 °C for the hydrogenolysis of PECHD. Complete PET conversion was

achieved, with 82% yield of CHDM and the formation of 4-methyl-1-cyclohexanemethanol (4-MCHM) as a byproduct. To enhance CHDM selectivity, a two-stage one-pot mode was employed: hydrogenation of PET to PECHD at 120 °C followed by hydrogenolysis of PECHD to CHDM at 200 °C. This approach yielded a remarkable 95% CHDM yield. In this process, Pd/r-GO catalyzed the hydrogenation of the PET aromatic ring to PECHD, while og-CuZn catalyzed the C–O hydrogenolysis of PECHD to CHDM. The formation of 4-MCHM primarily resulted from the hydrogenolysis of PET over the og-CuZn catalyst, followed by hydrogenation over the Pd/r-GO catalyst at a high reaction temperature. Controlled experiments conducted by systematically substituting Pd with Ru or Cu with Co revealed that the Ru/r-GO + og-CuZn catalyst system exhibited higher selectivity toward C–C bond cleavage products, whereas the Pd/r-GO + og-CoZn catalyst system showed enhanced selectivity toward C–O bond cleavage products. These findings further support the critical role of the synergistic combination between Pd/r-GO and og-CuZn in achieving selective bond cleavage during the catalytic conversion of PET (Fig. 3a). The outstanding hydrogenation ability of Pd/r-GO can be attributed to the high degree of graphitization of the r-GO support, which enhances the interaction between the support and the PET aromatic rings through π–π interactions, facilitating efficient activation of PET on the catalyst surface. Additionally, the inert nature of Pd toward C–O hydrogenolysis is another reason for achieving a high CHDM yield. For the og-CuZn catalyst, the Cu–ZnO interface serves as the active site for C–O hydrogenolysis. The strong Lewis acid sites on the og-derived ZnO surface play a critical role in the effective adsorption and activation of ester compounds, as confirmed by TPD-MS and *in situ* diffuse reflectance infrared Fourier transform spectroscopy (DRIFTS) experiments. Moreover, the high abundance of defective metallic Cu sites is essential for effective hydrogenolysis of PECHD through facilitating H_2 dissociation. The hydrogenolysis mechanism of PECHD on the surface of og-CuZn proceeds through three sequential steps: (i) activation of the ester groups in PECHD on ZnO, facilitated by the presence of strong Lewis acid sites; (ii) dissociation of molecular hydrogen on defective Cu^0 sites; and (iii) spillover of atomic hydrogen onto the ZnO surface, followed by its attack on the activated ester groups (Fig. 3b). To address the separation challenges posed by high-boiling diol-based products (CHDM boiling point: 286 °C and EG boiling point: 197.3 °C), the authors introduced a third reaction stage at 220 °C for EG hydrogenolysis to yield volatile products such as ethanol, ethane, and methane while maintaining a high CHDM yield of 92%. Using this method, the authors scaled up the reaction to 10 g, achieving a high isolated yield of 87% CHDM with 99% purity *via* simple filtration, evaporation, and vacuum distillation. Notably, the CHDM product obtained exhibited a high *trans*/*cis* ratio of 4.09/1, significantly exceeding the commercial CHDM ratio of 3.14/1. This improved *trans*/*cis* ratio offers potential advantages for chain packing, crystallization capacity, and crystal perfection in the synthesis of novel polymers. Control experiments indicated that the transformation from *cis* to *trans* predominantly occurred during the hydrogenolysis of PECHD in the specific microenvironment of the Cu–ZnO interface formed in og-CuZn. Furthermore, this catalyst system can effectively convert various PET waste sources, including dyed PET bottles, PET strapping bands, and PET fabrics, into CHDM with yields ranging from 78% to 89%. However, the recyclability of the catalyst system is unknown.

5 Hydrogenolysis of PET to yield TPA

TPA is a monomer used in the production of PET and can be produced *via* hydrolysis in neutral, acidic, or basic media.[19–22] However, this process suffers from the formation of side products that are difficult to separate and it requires large amounts of solvent.[19–22] In this context, hydrogenolysis offers a feasible approach for converting PET into TPA under neat

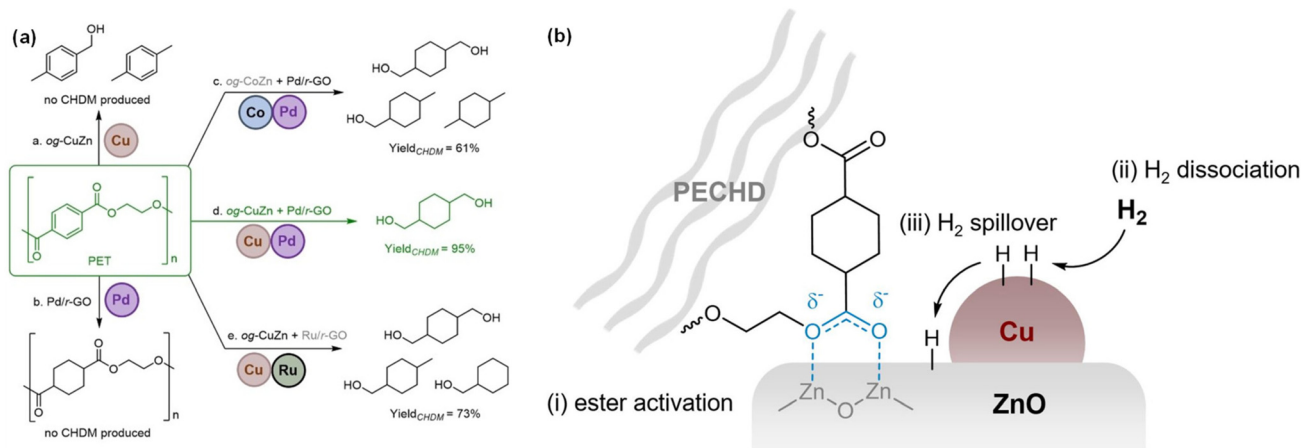

Fig. 3 (a) Controlled experiments replacing Pd/r-GO and og-CuZn with other catalysts. (b) Reaction mechanism for the hydrogenolysis of PECHD on the surface of og-CuZn. Reproduced with permission.[28] Copyright 2024, Wiley-VCH.

conditions. The yield of TPA through the hydrogenolysis method can reach up to 98% when recyclable heterogeneous catalysts are employed. This method eliminates the need for solvents and facilitates the recovery of the TPA product, thereby enhancing its environmental sustainability and practical feasibility. The critical step in producing TPA from PET involves cleavage of the C_{alkoxy}–O bond within the PET ester group. Recently, Mo-based catalysts[68,69] and Pd/C combined with a Lewis acid catalyst[70] or ionic liquid[71] have been developed, achieving high yields of TPA (Table 4). The mechanism for breaking the C_{alkoxy}–O bond involves either retro-hydroalkoxylation or nucleophilic substitution by halide anions, depending on the specific catalyst system employed.

The Marks group pioneered the hydrogenolysis of PET to TPA and ethylene by using a carbon-supported single-site molybdenum-dioxo catalyst (C/MoO_2) under 1 atm of H_2 (Scheme 7, Route I).[69] A TPA yield of 90% was achieved at 260 °C after 24 h. Moreover, this catalyst can effectively handle waste beverage bottle PET or a PET + polypropylene (PP) mixture, achieving complete PET deconstruction and quantitative TPA isolation. Mechanistic studies using a model diester, 1,2-ethanediol dibenzoate, indicate that the reaction proceeds through initial retro-hydroalkoxylation/β-C–O scission followed by hydrogenolysis steps (Fig. 4a). Specifically, the C═O and alkoxyl O groups of 1,2-ethanediol dibenzoate bind to Mo, forming a well-precedented hexacoordinate Mo–dioxo complex. This complex subsequently undergoes β-C–O scission to generate benzoic acid and vinyl benzoate. Hydrogen then adds across the Mo═O bond, releasing benzoic acid and yielding a Mo–vinyl benzoate complex. Both Mo–OH and Mo–H moieties can react with vinyl benzoate. In the case of Mo–OH, the formation of benzoic acid and ethylene involves nucleophilic attack and β-extrusion. For Mo–H moieties, the C═C bond of vinyl benzoate inserts into the Mo–H bond, forming a metal alkyl intermediate that undergoes β-elimination to produce ethylene and a C/Mo(═O)OH(OCOPh) species. After β-elimination, benzoic acid is generated, completing the catalytic cycle. The catalyst can be easily recycled without losing activity, maintaining an average TPA yield of 90% over four consecutive runs. To further enhance the catalytic efficiency, Cai *et al.* developed a bimetallic CoMo@NC catalyst derived from Mo@ZIF-CoZn for the direct hydrogenolysis of PET to TPA.[68] This catalyst achieves an impressive TPA yield of 91% within 10 h under 1 atm H_2 pressure and solvent-free conditions. The reaction mechanism involves β-C–O scission followed by hydrogenolysis, consistent with the pathway proposed by Marks' group. The incorporation of metallic Co promotes hydrogen activation, thereby significantly accelerating the reaction rate.

To further enhance the yield of TPA, Marks' group developed a catalytic system consisting of Pd/C and $Hf(OTf)_4$ for the hydrogenolysis of polyethylene terephthalate (PET) to TPA and ethane[70] (Scheme 7, Route II). Under solvent-free conditions, this system achieved a remarkable near-quantitative yield within 24 h at 265 °C under 1 atm H_2. Unlike C/MoO_2 catalysts that can independently catalyze hydrogenolysis reactions, the synergy between $Hf(OTf)_4$ and Pd/C is essential for efficient PET C–O bond hydrogenolysis and TPA formation. A combined experimental study using 1,2-ethanediol dibenzoate as a model compound, along with density functional theory (DFT) mechanistic analyses, revealed that the Lewis acidic $Hf(OTf)_4$ catalyst facilitates a mildly exergonic retro-hydroalkoxylation reaction (Fig. 4b). In this process, an alkoxy C–O bond is initially cleaved to generate carboxylic acid and ethylene. This step is coupled in tandem with a significantly exergonic olefin hydrogenation reaction catalyzed by Pd/C, driving the overall reaction forward. Notably, this catalytic system demonstrates versatility in converting various PET waste sources, including drinking bottles, shirts, and pillow stuffing, into TPA with yields reaching up to 97%.

The combination of an ionic liquid, 1-butyl-2,3-dimethylimidazolium bromide, and a Pd/C catalyst can also enable the hydrogenolysis of PET into TPA and ethane[71] (Scheme 7, Route II). This catalytic system achieves a high yield of TPA (85%) at

Table 4 Hydrogenolysis of PET over different catalysts to yield TPA

Entry	Catalysts	T (°C)	P_{H_2} (MPa)	t (h)	Yield (%)	Ref.
1	C/MoO_2	260	0.1	24	87	69
2	CoMo@NC	260	0.1	10	91	68
3	Pd/C + $Hf(OTf)_4$	180	0.1	24	98	70
4	Pd/C + [BMMIm]Br	180	5	48	85	71

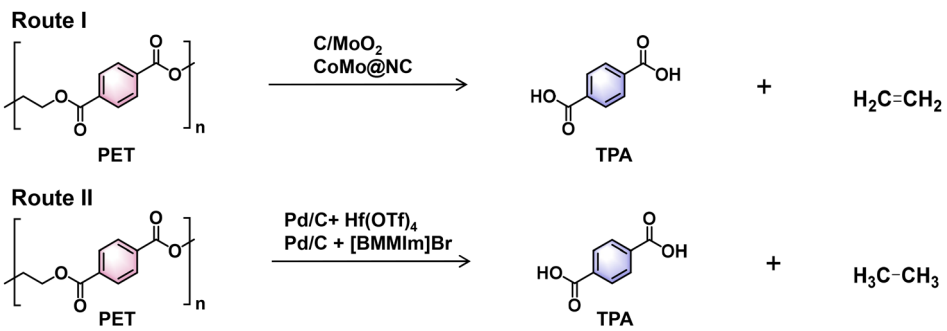

Scheme 7 Routes for the conversion of PET into TPA.

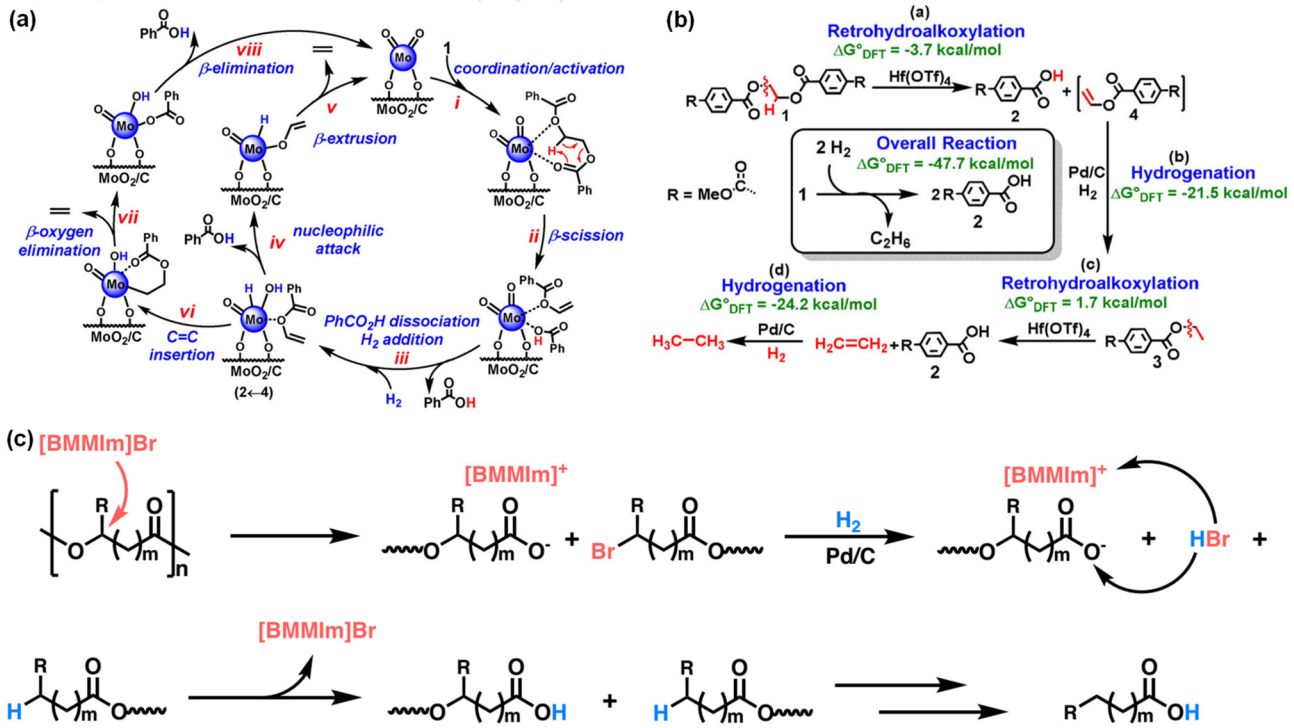

Fig. 4 (a) Reaction mechanism for the hydrogenolysis of 1,2-ethanediol dibenzoate over the C/MoO_2 catalyst. Reproduced with permission.[69] Copyright 2020, Wiley-VCH. (b) Reaction mechanism for the hydrogenolysis of 1,2-ethanediol dibenzoate over Pd/C + $Hf(OTf)_4$. Reproduced with permission.[70] Copyright 2021, Wiley-VCH. (c) Reaction mechanism for the hydrogenolysis of polyesters over Pd/C + [BMMIm]Br. Reproduced with permission.[71] Copyright 2024, Springer Nature.

a relatively low reaction temperature (180 °C), albeit under higher H_2 pressure (5 MPa) and longer reaction time (48 h) compared to the $Hf(OTf)_4$ and Pd/C system. In this system, the ionic liquid serves not only as a solvent but also catalyzes cleavage of the C_{alkoxy}–O bond *via* nucleophilic substitution by the halide anion (Br^-) of the ionic liquid. Nuclear magnetic resonance (NMR) and DFT analyses reveal that the hydrogen-bonding interaction between the ionic liquid and the ester group in PET enhances the nucleophilicity of the halide anion and activates the C_{alkoxy}–O bond. Furthermore, the reaction activity is strongly correlated with the high nucleophilicity index of the ionic liquid. In this context, the high performance of the Pd/C + [BMMIm]Br catalytic system can be attributed to the efficient cleavage of the ester C_{alkoxy}–O bond, which is facilitated by the nucleophilic attack of the Br^- anion on the carbon atom within the C_{alkoxy}–O bond (Fig. 4c). After cleavage of the C_{alkoxy}–O bond, two intermediates—the bromide and carboxylate anion—are formed. The carboxylate anion is stabilized by the ionic liquid cation. Subsequently, the bromide intermediate undergoes hydrodebromination over Pd/C with H_2, producing HBr and alkyl-terminated species. The carboxylate anion is then acidified by the HBr generated, yielding carboxylic acid-terminated species while regenerating the ionic liquid. Through this mechanism, TPA can be continuously formed *via* the sequential cleavage of C_{alkoxy}–O bonds linked to each ester group in PET.

6 Selective asymmetric hydrogenolysis of PET to yield MMB and PTA

The asymmetric hydrogenolysis of PET can produce methyl *p*-methyl benzoate (MMB)[72] and *p*-toluic acid (PTA),[73] both of which are high-value oxygenated products. For instance, MMB is priced at nearly twice the value of DMT, whereas PTA is valued at approximately three times the price of TPA. Nevertheless, the strong π–π conjugation effects of the benzene rings and the symmetrical arrangement of carboxyl groups significantly hinder the asymmetric activation and transformation of critical functional sites. To address these intrinsic challenges, it is essential to design highly efficient, targeted, and selective catalytic systems capable of overcoming these barriers.

6.1 Tandem methanolysis and hydrogenolysis to yield MMB

MMB is widely used in the production of fine chemicals, including pharmaceuticals, agrochemicals and dyes.[74,75] The conventional preparation method for MMB involves the oxidation of PX to PTA and subsequent esterification with methanol (Scheme 8, Route I).[76–78] However, its application is hindered by issues including poor selectivity towards MMB and high-cost noble-metal catalysts. To address this challenge, Li's

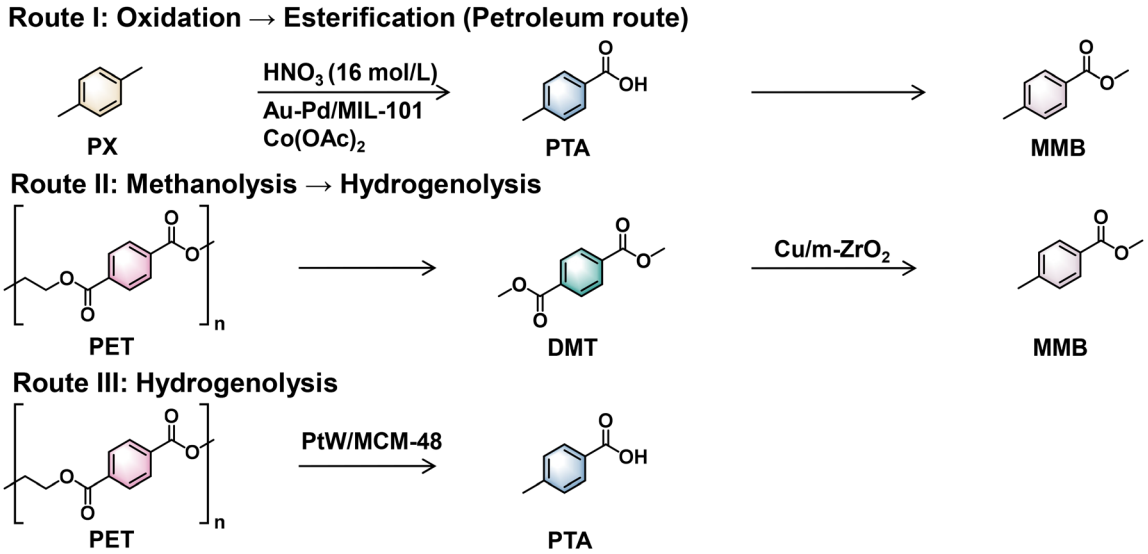

Scheme 8 Routes for the conversion of PET into PTA and MMB.

group recently reported a two-step strategy for the semi-HDO of PET to produce MMB.[72] This innovative approach involves the initial methanolysis of PET to DMT, followed by the subsequent partial HDO of DMT to MMB over Cu/m-ZrO_2 and La_2O_3 modified Cu/m-ZrO_2 catalysts in a flow reactor (Scheme 8, Route II). The catalysts exhibit a high selectivity (86%) towards MMB along with a moderate conversion of DMT (58%) at 180 °C. Doping with La_2O_3 significantly enhanced the stability of the catalyst by effectively suppressing copper nanoparticle sintering, resulting in a continuous reaction lasting for 120 h. The phase structure of the ZrO_2 support plays a crucial role in regulating the distribution of products. Specifically, the monoclinic ZrO_2 support (m-ZrO_2) gave high selectivity towards MMB (86%), while the tetragonal ZrO_2 support (t-ZrO_2) exhibited good selectivity for PX (75%) and low selectivity for MMB (23%). In comparison with t-ZrO_2, m-ZrO_2 possesses weaker Lewis acid sites and a lower adsorption ability towards DMT and MMB, which lead to the preferential production of MMB. These results can be confirmed by pyridine FT-IR and methyl acetate TPD-MS for m-ZrO_2 and t-ZrO_2. Furthermore, DFT calculations indicate that hydrogen can be readily dissociated into H* species on Cu^0 active sites. The DMT molecule chemisorbs onto the Cu/m-ZrO_2 ($\bar{1}11$) and Cu/t-ZrO_2(111) surfaces, where it can subsequently react with H* species, leading to the first C–O bond cleavage with relatively low free energy barriers of 1.16 eV on Cu/m-ZrO_2 ($\bar{1}11$) and 0.7 eV on Cu/t-ZrO_2(111). However, the second C–O bond cleavage exhibits a significantly higher energy barrier on Cu/m-ZrO_2($\bar{1}11$) (2.93 eV) compared to Cu/t-ZrO_2(111) (1.57 eV), further supporting the notion that m-ZrO_2 as a support material promotes selective asymmetric hydrogenolysis to yield MMB (Fig. 5a and b). It is noted that the distribution of products is also highly influenced by the reaction temperature. Lower reaction temperatures (150–180 °C) enable a high selectivity of MMB (86–93%) to be achieved, while higher reaction temperatures (200 °C) result in a significant yield of *para*-xylene (82%). The authors only demonstrate the methanolysis of various PET plastic wastes, including PET bottles, shirts, soundproof cotton and film, to DMT with exceptional yields. However, there is a lack of investigations into the semi-HDO of thus-obtained DMT to MMB over Cu/m-ZrO_2. Additional studies on enhancing the catalytic activity and process applicability for semi-HDO of DMT derived from various PET plastic wastes are needed.

6.2 Direct hydrogenolysis to yield PTA

PTA is extensively utilized in photographic materials, phosphoramidate fungicides, and organic synthesis.[79,80] The industrial production of PTA generally entails the oxidation of PX using concentrated nitric acid, a process that not only leads to severe equipment corrosion but also releases nitrogen oxides, thereby worsening environmental pollution (Scheme 8, Route I).[81] Moreover, the partial oxidation of PX catalyzed by cobalt naphthenate can produce PTA; however, this method suffers from a low yield of PTA (17.8%) and the inability to recycle the catalyst.[82]

Recently, Mei's group reported a novel one-step approach for the selective hydrogenation of waste PET to PTA using a bifunctional PtW/MCM-48 catalyst (Scheme 8, Route III).[73] The employment of phosphotungstic acid (PWA) as the acidic medium is crucial for achieving a high yield of PTA; this can be attributed to its strong proton-donating ability that facilitates the initial depolymerization of PET. The optimal reaction conditions were identified as pH 2, 260 °C, and 2 MPa H_2. A remarkable yield of PTA (53.4%) was achieved alongside a moderate yield of PX (36.4%). A kinetic study on PET conversion revealed that the reaction pathway over PtW/MCM-48 involved the depolymerization of PET to TPA in an acidic aqueous solution, followed by the selective hydrogenation of TPA to 4-(hydroxymethyl)benzoic acid (HMBA), which was sub-

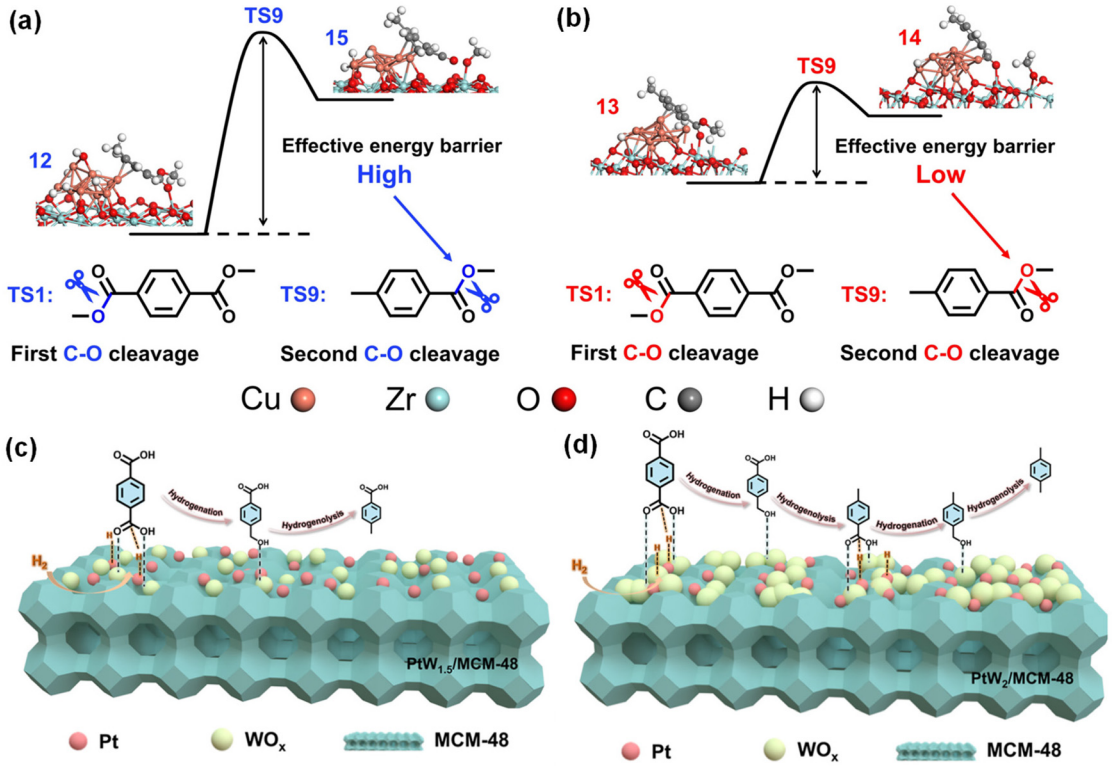

Fig. 5 Reaction diagram [energy (*E*)] for DMT hydrogenation on the Cu/m-ZrO_2 ($\bar{1}11$) (a) and Cu/t-ZrO_2(111) (b) catalyst models. Reproduced with permission.[72] Copyright 2024, Wiley-VCH. Reaction mechanism for the hydrogenolysis of PET to PTA and PX over the $PtW_{1.5}$/MCM-48 (c) and PtW_2/MCM-48 (d) catalysts. Reproduced with permission.[73] Copyright 2024, American Chemical Society.

sequently converted into PTA. PX is formed *via* the overhydrogenolysis of PTA. Characterization studies revealed that the incorporation of WO_x species significantly improved the dispersion of Pt nanoparticles, with strong interactions observed between Pt and WO_x. Notably, the WO_x species were present predominantly as polytungstates with a low degree of polymerization. The introduction of WO_x facilitated the vertical adsorption of TPA onto the active sites of PtW/MCM-48, thereby suppressing benzene ring hydrogenation and promoting the efficient hydrolysis of PET to TPA. Subsequently, adsorbed TPA underwent selective hydrogenation to PTA under the synergistic effects of Pt^0 and H_2. The Pt/W molar ratio was identified as a key parameter in controlling the extent of deoxygenation. When the Pt/W molar ratio was 1.5, the PtW1.5/MCM-48 catalyst exhibited a moderate $W^{5+}/(W^{5+} + W^{6+})$ content and predominantly weak acidic sites, which favored the desorption of PTA and resulted in high PTA selectivity (Fig. 5c). In contrast, at a Pt/W molar ratio of 1 : 2, excess WO_x species with abundant medium- to strong acidic sites led to the re-adsorption of PTA, making it difficult for the carboxyl groups to remain intact. This promoted further deoxygenation to PX (Fig. 5d). DRIFTS and TPD-MS studies using acetic acid as a probe molecule over $PtW_{1.5}$/MCM-48 and PtW_2/MCM-48 provided evidence that excess WO_x species on PtW_2/MCM-48 strongly adsorbed the initial hydrogenolysis product, PTA, thereby promoting its over-hydrogenolysis to PX. DFT calculations further revealed that the adsorption energies of PTA and PX on the W_4O_7/Pt(111) surface (a model for PtW_2/MCM-48) were higher than those on the W_3O_7/Pt(111) surface (a model for $PtW_{1.5}$/MCM-48), indicating that PTA was less likely to desorb from PtW_2/MCM-48. These findings demonstrate that the controlled adsorption behavior of PTA on the PtW/MCM-48 catalyst, regulated by adjusting the Pt/W ratio, is crucial for achieving high PTA yields. The developed $PtW_{1.5}$/MCM-48 catalyst demonstrated broad applicability, enabling the conversion of various PET waste plastics, such as polyester rope, seal bags, water bottles, colored snakeskin ropes, trays, ribbons, and terylene cotton, into PTA with yields ranging from 43.9% to 54.8%. Furthermore, this catalyst could be reused for five consecutive cycles after regeneration *via* calcination and re-reduction.

TEA and LCA analyses were conducted to evaluate and compare the economic viability and environmental impact of the one-pot hydrogenolysis process for converting PET into TPA with those of the conventional naphtha-based three-step process. The TEA results indicated that the PET-based one-pot process generated a gross profit of $8446 per ton of PTA, surpassing the naphtha-based three-step process, which yielded $4806 per ton. This economic advantage is attributed to higher PTA production, fewer byproducts, greater process efficiency, reduced catalyst consumption, and a simplified operational procedure. In addition, LCA results demonstrated

that the total global warming potential (GWP) of the PET-based one-pot process (5.18 kg CO_2-eq per kg) was lower than that of the naphtha-based three-step process (5.97 kg CO_2-eq per kg). Moreover, the GWP of the one-pot process is significantly lower than alternative PET disposal methods such as direct incineration or landfilling (10.51 kg CO_2-eq per kg), as well as conventional hydrolysis routes for producing TPA and EG (5.60 kg CO_2-eq per kg). These findings underscore the substantial environmental benefits associated with the one-pot hydrogenolysis process.

7 Hydrodeoxygenation of PET to yield aromatics

HDO of PET without aromatic ring saturation can produce BTX aromatics (benzene, toluene, and xylene). These aromatic compounds are crucial intermediates in the chemical industry. Notably, PX serves as a key starting material for TPA monomer production *via* conventional technology, which is subsequently used for PET synthesis, thereby establishing a closed-loop PET recycling pathway. The primary challenge in achieving selective HDO of PET to aromatics involves selectively breaking the C–O bond while preserving the integrity of the C–C bond and aromatic ring structure. BTX production from PET can be realized through HDO processes with or without an external hydrogen supply (Scheme 9). Processes without external hydrogen typically utilize hydrogen generated from methanol decomposition or ethylene glycol aqueous phase reforming (Scheme 9, Route III). Catalysts employed for BTX production from PET include precious metal catalysts (*e.g.*, Ru/Nb_2O_5,[29] Ru/TiO_2[83,84]) and base metal catalysts (*e.g.*, Co/TiO_2,[85] $Co–ReO_x/Al_2O_3$,[86] $Cu/ZnO/Al_2O_3$,[87] Cu/SiO_2,[88] $Cu/ZnZrO_2$[89]). The performances of these catalysts are summarized in Table 5.

7.1 HDO of PET with hydrogen to yield aromatics

Wang *et al.* pioneered the HDO of PET to aromatics using a Ru/Nb_2O_5 catalyst (Scheme 9, Route I).[29] Under conditions of 200 °C, 0.3 MPa H_2, and 12 h in water as the solvent, an aromatic product yield of 80.6% was achieved. Among these products, PX was the predominant component in a yield of 62%. Additionally, this catalyst demonstrated its versatility by converting Coca-Cola bottles into aromatics with a yield as high as 71.3%. When octane was employed as the solvent under conditions of 280 °C, the total yield of BTX reached 83.6%, comprising 14% benzene, 41% toluene, and 45% PX. Notably, the reaction temperature in octane as the solvent (280 °C) was higher than that in water (200 °C). Remarkably, this catalyst could also convert mixed aromatic plastics, including PET, polystyrene (PS), polyphenylene oxide (PPO), and polycarbonate (PC), into aromatics with a yield of 78.9%. The catalyst exhibited excellent durability, maintaining consistent yields of aromatics after three cycles following regeneration *via* calcination and reduction. Systematic characterization studies revealed that small Ru clusters with low coordination numbers (C.N. = 5–6) were evenly dispersed on the Nb_2O_5 support.

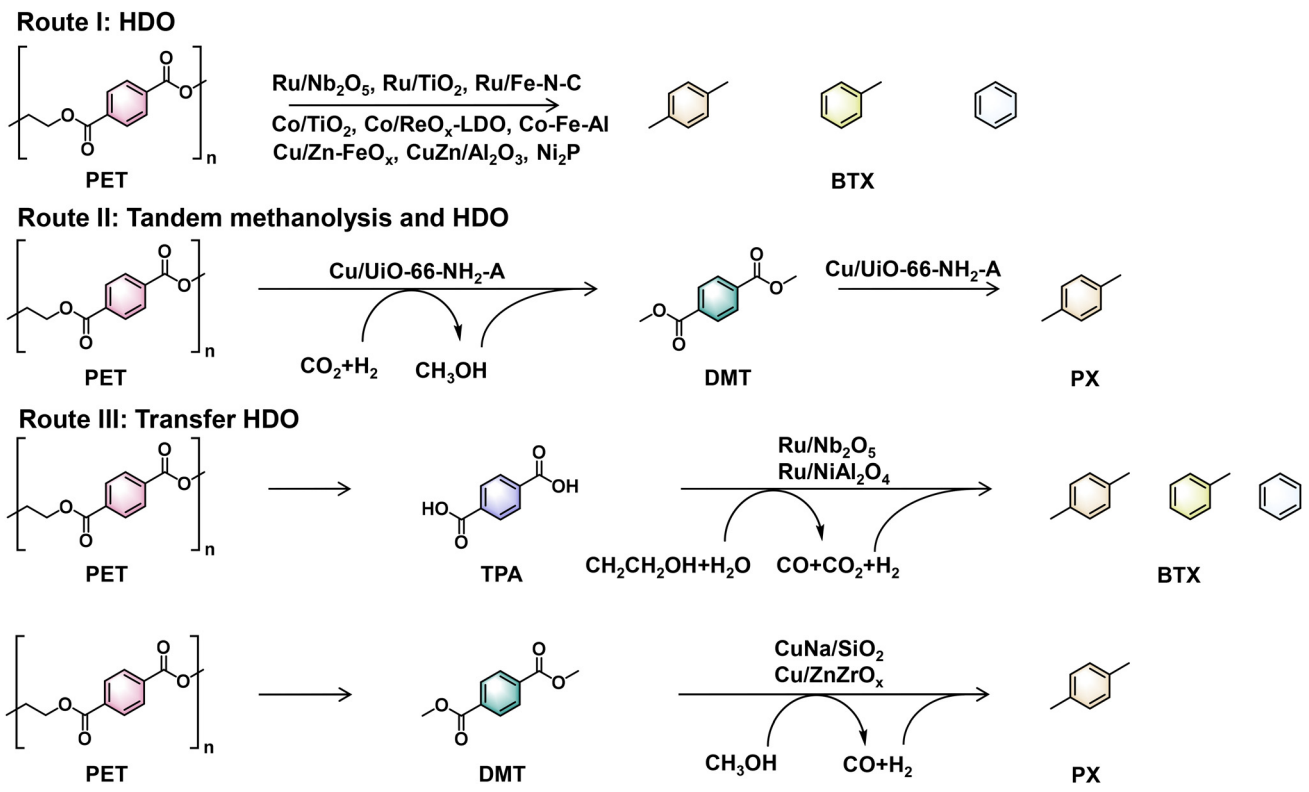

Scheme 9 Routes for the conversion of PET into aromatics.

Table 5 HDO of PET over different catalysts to yield aromatics

Entry	Method	Catalysts	Products	Solvent	T/°C	P_{H_2}/MPa	t/h	Yield/%	Ref.
1	HDO	Ru/Nb_2O_5	BTX	Octane	280	0.5	8	83.6	29
2	HDO	Ru/Nb_2O_5	BTX	H_2O	200	0.3	12	82.9	29
3	HDO	Ru/TiO_2	BTX	H_2O	230	0.3	12	77	83
4	HDO	Ru/TiO_2	BTX	H_2O/dodecane	220	0.1	12	99	84
5	HDO	Ru/Fe–N–C	BTX	Dodecane	350	5	4	97.1	90
6	HDO	Co/TiO_2	BTX	Dodecane	340	3	24	78.9	85
7	HDO	Co/ReO_x-LDO	PX	2-Propanol	210	3	4	71.7	86
8	HDO	Co–Fe–Al	PX	1,4-Dioxane	210	4	10	99.0	91
9	HDO	$Cu/Zn–FeO_x$	PX	1,4-Dioxane	200	4	8	98.6	92
10	HDO	$CuZn/Al_2O_3$	PX	1,4-Dioxane	240	3	8	99.8	87
11	HDO	Ni_2P	BTX	Dodecane	400	9	6	93.0	93
12	HDO	Cu/UiO-66-NH_2-A	PX	—	250	3 (P_{CO_2} : P_{H_2} = 1 : 3)	36	89.5	94
13	Transfer HDO	Ru/Nb_2O_5	BTX	H_2O	220	—	12	91.3	95
14	Transfer HDO	$Ru/NiAl_2O_4$	BTX	H_2O	220	—	12	64.0	95
15	Transfer HDO	$CuNa/SiO_2$	PX	Methanol	210	—	6	100	88
16	Transfer HDO	$Cu/ZnZrO_x$	PX	Methanol/dioxane	240	3	16	63	89

These small Ru nanoclusters acted as hydrogenation sites while effectively suppressing the adsorption of aromatic rings, thereby achieving high selectivity towards aromatics. On the other hand, oxophilic NbO_x species played a critical role in the adsorption and activation of C–O bonds. The synergistic effect between the small Ru clusters and the oxophilic NbO_x species was responsible for the catalyst's high activity and selectivity towards aromatics (Fig. 6a). The catalyst can be recycled for three times with consistent yields of aromatics after regeneration by calcination and reduction.

Zhang *et al.* demonstrated that Ru/TiO_2 exhibited activity for the HDO of PET to aromatic compounds when the Ru particle size was carefully controlled.[83] When the Ru particle size was approximately 1.1 nm with a coordination number of around 5.0, the catalyst, which predominantly featured edge/corner sites, achieved a total BTX yield of 77% under conditions of 280 °C, 0.3 MPa H_2 for 12 h. Conversely, larger Ru/TiO_2 particles yielded more ring hydrogenation and ring-opening products (Fig. 6b). DFT calculations and isotopic labeling experiments revealed that the upright adsorption configuration of aromatic intermediates on under-coordinated Ru sites was more favorable than on well-coordinated Ru terrace sites. Consequently, aromatic ring saturation can be effectively suppressed (Fig. 6b). This finding aligns with the case of the Ru/Nb_2O_5 catalyst, which also possesses small Ru nanoclusters with a coordination number of 5–6. On the other hand, ring-opening reactions are more feasible on terrace sites, which are more abundant in larger Ru nanoparticles. The activity of this catalyst can be retained for three consecutive runs and no obvious sintering or leaching were observed for each run. Jae *et al.* also reported that Ru/TiO_2 was active for the HDO of PET to BTX, achieving a BTX yield of up to 99% under mild reaction conditions (220 °C, 1 MPa H_2, 12 h) in a water–dodecane biphasic solvent system.[84] They further found that the Ru particle size of Ru/TiO_2 catalysts significantly influenced product distributions. Ru nanoclusters with sizes ranging from 0.8 to 1.2 nm possess an enhanced proportion of under-coordinated corner and edge sites, favoring the production of BTX, particularly alkyl aromatics. Smaller Ru nanoclusters (<0.8 nm) promote decarboxylation reactions, while larger Ru particles (>2 nm) lead to ring-saturated products such as cyclohexane. These findings are consistent with those reported by Zhang *et al.*[83] Additionally, they also found that strong metal–support interactions (SMSIs) in Ru/TiO_2 catalysts played a crucial role in determining the HDO activity of PET. The Ru/TiO_2 catalyst reduced at 400 °C with a moderate level of SMSIs proved to be the most active. The formation of Ru/TiO_x interfaces enables the capture of oxygen from carbonyl groups, facilitating direct C–O hydrogenolysis. The TiO_2 support facilitates the formation of stable emulsions, and larger TiO_2 particles reduce the distance between O/W emulsion droplets, enabling rapid H_2 transport and accelerating the hydrogenation and dehydration of mono-oxygenated aromatic intermediates into aromatics (Fig. 6c–e).

In addition to Ru/Nb_2O_5 and Ru/TiO_2 catalysts, the Ru/Fe–N–C catalyst has also been demonstrated to be effective at the HDO of PET to BTX, achieving a total yield of 96%.[90] Among the aromatic products, PX can reach a yield of up to 82.6% at 350 °C, 1 MPa H_2 for 4 h, which represents the highest PX yield among Ru-based catalysts. The formation of $Ru–N_x$ species plays a critical role in enabling the vertical adsorption of the C=O bond in the ester group, thereby leading to high selectivity towards aromatics. The formation of aromatics proceeded through the successive C–O bond cleavage of the ester group of PET followed by hydrogenation (Fig. 6f). In contrast, in the absence of $Ru–N_x$ species, high yields of cycloalkanes are obtained. However, the stability of the catalyst is not satisfactory due to the aggregation of Ru nanoparticles.

To reduce the high cost associated with Ru-based catalysts, non-noble Co-based metallic catalysts have also been developed for the HDO of PET to BTX. Yan's group was the first to discover that a Co/TiO_2 catalyst was effective at the HDO conversion of PET to aromatics, achieving a yield of 78.9% under conditions of 320 °C, 3 MPa H_2 for 24 h.[85] However, the catalyst exhibited poor stability, with the BTX yield decreasing to 35% due to the formation of an inactive $CoTiO_3$ phase. To

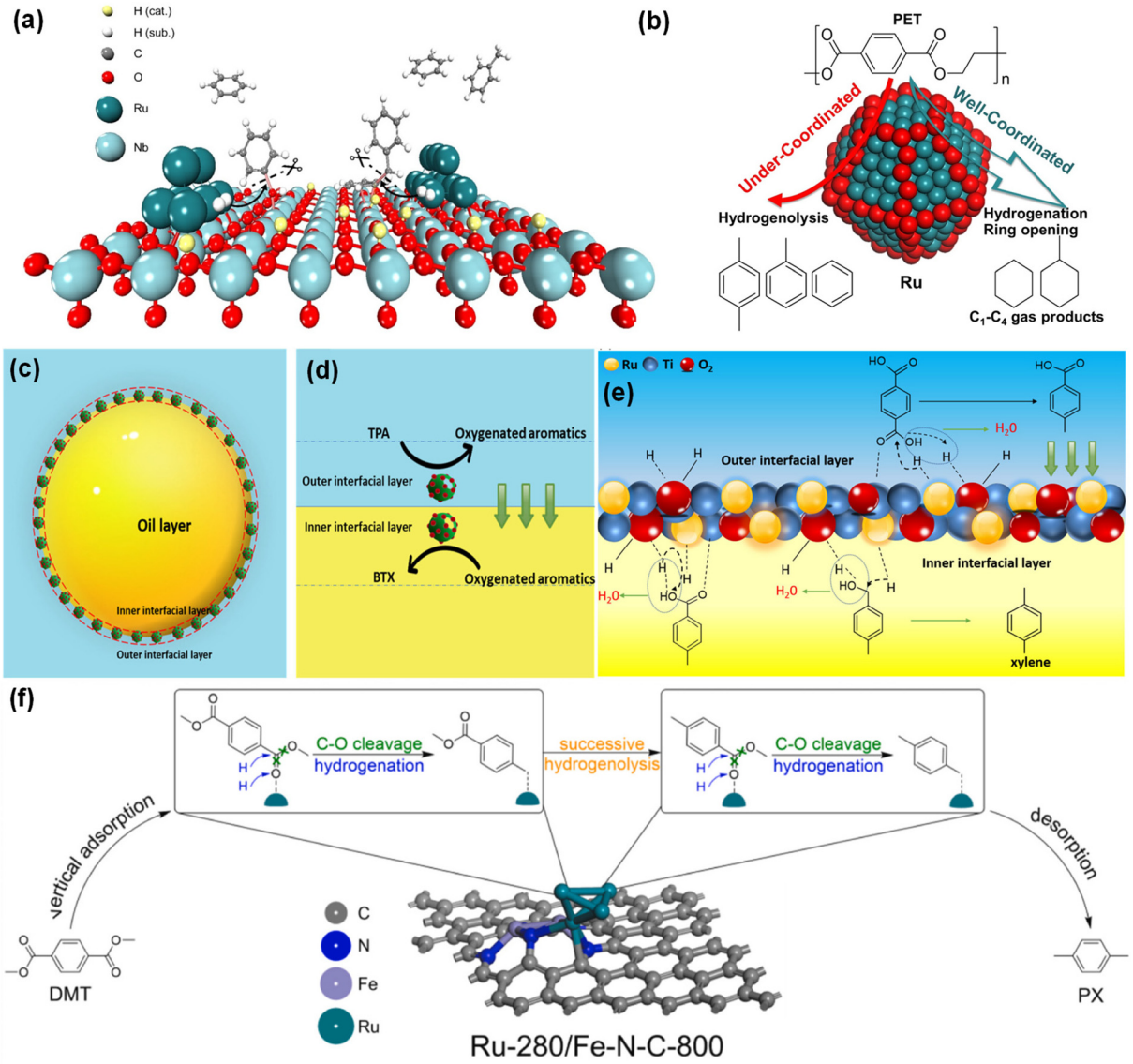

Fig. 6 (a) Proposed mechanism for catalytic C–O/C–C cleavage over Ru/Nb_2O_5. Reproduced with permission.[29] Copyright 2024, Wiley-VCH. (b) Proposed reaction pathways for PET hydrogenolysis dictated by the Ru coordination environment of Ru/TiO_2. Reproduced with permission.[83] Copyright 2024, Wiley-VCH. (c) Liquid–liquid interfacial catalysis effect; (d) schematic illustration of the inner and outer interfacial layers at the oil–water interface. (e) Reaction scheme for the hydrogenation of PET on the surface of Ru particles located in the outer and inner interfacial layers of a Pickering emulsion. Reproduced with permission.[84] Copyright 2025, The Royal Society of Chemistry. (f) The proposed reaction pathway for HDO of DMT over the Ru/Fe–N–C catalyst. Reproduced with permission.[90] Copyright 2024, Elsevier.

further enhance catalyst stability, Nie *et al.* developed a novel Co/ReO_x-LDO catalyst, which afforded a PX yield of 71.7% at 210 °C, 3 MPa H_2, and 4 h.[86] Remarkably, this catalyst demonstrated excellent stability over four cycles, maintaining nearly constant PX yields. During the HDO of PET to aromatics, cleavage of the acyl C–O bond in the ester group is the rate-determining step. Characterization studies revealed that partially reduced ReO_x species were located adjacent to Co metallic particles with strong interactions. This strong interaction facilitates the hydrogenolysis of the acyl C–O bond. Additionally, small-sized Co nanoparticles with higher charge density effectively suppress aromatic ring hydrogenation and C–C bond cleavage, while the adjacent ReO_x species promote hydrogen spillover, thereby enhancing catalyst activity. To further improve the PX yield, Hu *et al.* developed a Co–Fe–Al catalyst for the HDO of PET and Coca-Cola bottles, achieving a PX yield of 99% at 210 °C, 4 MPa H_2 for 10 h.[91] The addition of Fe enhances the catalyst's ability to adsorb and activate oxygenate intermediates while suppressing benzene ring hydrogenation. As a result, the catalyst exhibits high selectivity towards aromatics. Furthermore, this catalyst demonstrated excellent stability over five consecutive runs.

Copper-based catalysts, including $Cu/Zn–FeO_x$[92] and $CuZn/Al_2O_3$,[87] have been reported to exhibit remarkable activity for

the HDO of PET to PX. The Cu/Zn–FeO_x catalyst achieves a PX yield of 98.6% at 200 °C, 4 MPa H_2 for 8 h, while the CuZn/Al_2O_3 catalyst yields 99.8% PX under conditions of 230 °C, 3 MPa H_2 for 8 h. During the HDO of PET to PX over copper-based catalysts, the degradation of PET primarily involves the cleavage of ester bonds to alcohols, followed by the hydrogenolysis of C–O bonds in these alcohols to form aromatics. 4-Methyl benzyl alcohol has been identified as a key reaction intermediate, with its hydrogenolysis representing the rate-determining step. Characterization studies revealed that the incorporation of Zn in the Cu/Zn–FeO_x catalyst induced abundant Lewis acidic sites, promoting the dispersion and reduction of Cu species. These Lewis acidic sites induced by Zn played a crucial role in the adsorption and activation of oxygenated intermediates, thereby enhancing C–O bond hydrogenolysis. In the case of the CuZn/Al_2O_3 catalyst, the synergistic effect between Cu^0 and Cu^+ species contributes to its superior HDO performance. Specifically, Cu^0 species activate hydrogen, while Cu^+ species facilitate the activation of C–O bonds. The presence of Zn enhances the dispersion of Cu^0 and increases the Cu^+/Cu^0 ratio, thereby improving both the activity and selectivity of the catalyst. Compared to the Cu/Zn–FeO_x catalyst, the CuZn/Al_2O_3 catalyst demonstrates excellent stability, with PX yields remaining nearly constant after five cycles.

Golubeva *et al.* employed a heterogeneous nickel phosphide catalyst for the HDO of PET waste bottles to yield BTX.[93] After systematically optimizing the reaction conditions, the highest BTX yield reached 93% under conditions of 400 °C, 9 MPa H_2, and 6 h. The active site was identified as the Ni_2P phase, which formed *in situ* during the reaction. The acidic sites of the catalyst facilitated the depolymerization of PET. The presence of $Ni^{\delta+}$ species on the catalyst surface promoted decarboxylation reactions, resulting in higher selectivity towards benzene and toluene compared to PX. However, the catalyst exhibited poor stability, as evidenced by a decrease in PET conversion after the third run, potentially due to the reduced content of the Ni_2P phase in the catalyst sample.

7.2 Tandem methanolysis and HDO of PET with hydrogen and CO_2 to yield aromatics

The tandem methanolysis and HDO of PET to yield aromatics can be achieved under a H_2 and CO_2 atmosphere (Scheme 9, Route II). Methanol generated *via* CO_2 hydrogenation serves as the synthon for subsequent PET methanolysis to DMT. DMT formed can then undergo hydrogenolysis to produce PX. To realize this process, Li *et al.* designed a well-defined Cu/UiO-66-NH_2-A catalyst with abundant atomic Cu–O–Zr sites for catalyzing this cascade reaction.[94] Under optimized reaction conditions (250 °C, 3 MPa gas mixture of $CO_2:H_2$ = 1 : 3 for 36 h), 89.5% PX yield was achieved. Characterization studies confirmed that the precisely constructed Cu–O–Zr sites were the active sites for catalyzing the cascade reactions. These Cu–O–Zr sites enable the catalyst to exhibit superior adsorption and activation capabilities for CO_2 and H_2, as well as enhanced hydrogenation activity through hydrogen spillover, driving the reaction forward. Mechanistic studies revealed that CO_2 hydrogenation proceeded *via* the carbonate → bicarbonate → formate → H_2CO_2* and H_3CO* pathway (Fig. 7). In the HDO step, time-dependent reactions and *in situ* DRIFTS experiments identified methyl 4-(methylol)benzoate as the key intermediate. The C═O bond of this intermediate is adsorbed and activated by the Zr site, while hydrogen is activated by the Cu site. Subsequently, the C–O bond is cleaved to PX *via* 4-methylbenzyl alcohol as an intermediate (Fig. 7). The obtained Cu/UiO-66-NH_2-A catalyst can convert PET cups and lids into PX with yields ranging from 77.3% to 82.6%. However, the catalyst exhibits a poor cycling performance and stability, with PX yield decreasing to 50.5% after three cycles. X-ray photoelectron spectroscopy (XPS) analysis indicated that the reduced content of Cu^+ species after reaction was the primary cause of the decreased catalytic performance. Therefore, further improvement of the catalyst stability is necessary.

7.3 Transfer HDO of PET to yield aromatics

To mitigate the risks associated with handling hydrogen and reduce the high costs of H_2 usage, the HDO of PET to yield aromatics without an external hydrogen supply is a promising approach. In 2021, Wang *et al.* demonstrated for the first time the conversion of PET into benzene, toluene, and xylene (BTX) *via in situ* generated H_2 from ethylene glycol (EG) aqueous reforming reactions over Ru/$NiAl_2O_4$ or Ru/Nb_2O_5 catalysts[95] (Scheme 9, Route III). This process involves the hydrolysis of PET to TPA and EG, followed by EG reforming to generate H_2, and subsequently the hydrogenolysis/decarboxylation of TPA to BTX. The BTX yield can reach up to 91.3% under conditions of 220 °C, 3 MPa for 12 h. Compared to the Ru/$NiAl_2O_4$ catalyst, the Ru/Nb_2O_5 catalyst exhibited a higher selectivity towards alkyl aromatic products (toluene and *para*-xylene), achieving a yield of 66.7%. The $NiAl_2O_4$ and Nb_2O_5 supports play critical roles in catalyzing the hydrolysis reaction, while the hydrogenolysis/decarboxylation steps are identified as the rate-determining steps during this process. Characterization studies and control experiments revealed that the higher proportion of Ru^0 species on Ru/$NiAl_2O_4$ favored decarboxylation reactions, whereas the strong interaction between Ru and Nb_2O_5, combined with the high oxophilic nature of Nb_2O_5, led to enhanced hydrogenolysis activity. Furthermore, the catalyst can be regenerated and reused through reduction treatment. Additionally, the Ru/Nb_2O_5 catalyst has been successfully applied to convert various PET plastic waste streams, including Coca-Cola bottles, films, and textiles, into BTX with yields ranging from 81.6% to 93.3%.

Methanol can function as both a solvent and a hydrogen donor through its decomposition reaction. In 2022, Zhao *et al.* developed a CuNa/SiO_2 catalyst for the one-pot conversion of PET into PX and EG with quantitative yields under conditions of 210 °C for 6 h (Scheme 9, Route III).[88] The degradation of PET to PX involves tandem reactions: methanolysis of PET to DMT followed by HDO of DMT to PX, facilitated by *in situ* generated H_2 from methanol decomposition. The high Cu^+/Cu^0 ratio derived from sodium-doped copper silicate is critical for achieving an excellent performance. However, the catalyst

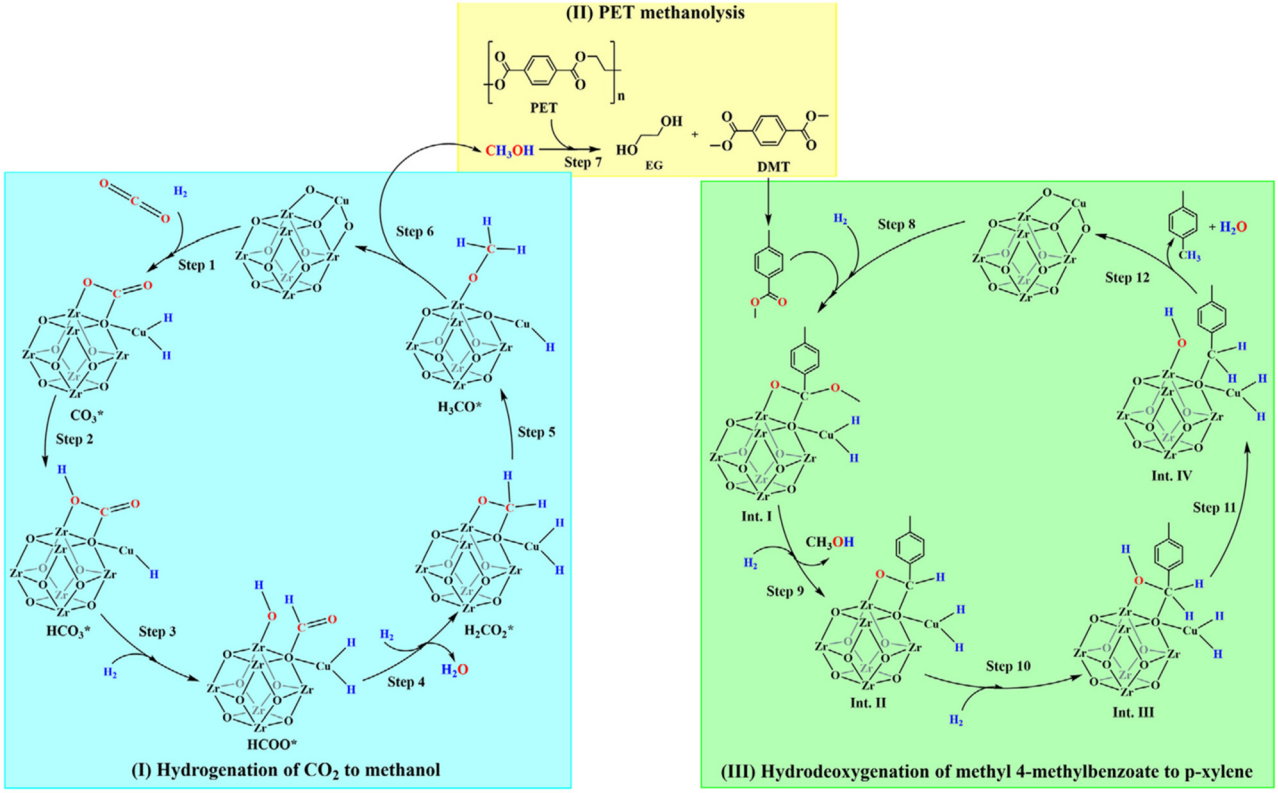

Fig. 7 Proposed reaction mechanisms over Cu/UiO-66-NH_2-A. Reproduced with permission.[94] Copyright 2025, Wiley-VCH.

cannot be reused due to the reduced Cu^+/Cu^0 ratio and copper sintering during the reaction process. Later, the Shetty group developed a $Cu/ZnZrO_x$ catalyst for the tandem methanolysis and transfer hydrogenolysis conversion of PET into PX.[89] Under conditions of 240 °C for 16 h, the yield of PX reached approximately 63%, which was lower than that achieved using the $CuNa/SiO_2$ catalyst. The reaction mechanism is similar to that over $CuNa/SiO_2$, involving methanolysis of PET to DMT and subsequent HDO of DMT to PX. However, unlike the $CuNa/SiO_2$ catalyst, which operates in condensed methanol solvent, vapor-phase methanol plays a crucial role in stabilizing surface H-coverage, thereby enhancing the reaction activity. The metal–support interfaces of the $Cu/ZnZrO_x$ catalyst are vital for the adsorption of methanol and DMT intermediates and for facilitating C–O bond hydrogenolysis, with cleavage of the acyl C–O bond of PET ester linkages being the rate-determining step. Although the catalyst's activity can be partially restored through calcination, further improvements are needed in future work.

8 Hydrodeoxygenation of PET to yield cycloalkanes

HDO of PET can yield cycloalkanes, including 1,4-dimethylcyclohexane (DMCH), methylcyclohexane, and cyclohexane. These cycloalkanes can serve as fuel components or liquid organic hydrogen carriers (LOHCs).[30,96,97] Among the cycloalkane products, DMCH is particularly desirable. The main challenge in achieving complete HDO of PET to DMCH lies in selectively cleaving the C–O bond while preserving the C–C bond. Recently, two distinct processes were reported for the production of cycloalkanes: multi-step and one-pot processes (Scheme 10). Catalysts used in these processes include metal–metal oxide catalyst systems (*e.g.*, Ru/TiO_2,[98,99] $Ru–ReO_x/SiO_2$,[30] $Ir–ReO_x/SiO_2$[100]) and metal–solid acid catalysts (*e.g.*, Ni/HZSM-5[101]). A comparison of the performances of these catalysts is summarized in Table 6. In the metal–metal oxide catalytic system, the mechanism of C–O hydrogenolysis is attributed to the synergistic effect between the metal oxide and the metal, wherein the partially reduced metal oxide is responsible for adsorbing and activating the C–O bonds, while the metal facilitates hydrogen activation. In the metal–solid acid catalytic system, the metal is primarily involved in hydrogenation and C–O bond hydrogenolysis, whereas the solid acid contributes to dehydration, thereby enhancing the overall HDO activity.

8.1 HDO of PET over noble metal catalysts to yield cycloalkanes

Li *et al.* pioneered the multi-step conversion of PET into C_7–C_8 cycloalkanes.[96] This process encompasses the methanolysis of PET to DMT, the hydrogenation of DMT to DMCD, and the subsequent HDO of DMCD to C_7–C_8 cycloalkanes (Scheme 10, Route I). The methanolysis of PET to DMT was conducted

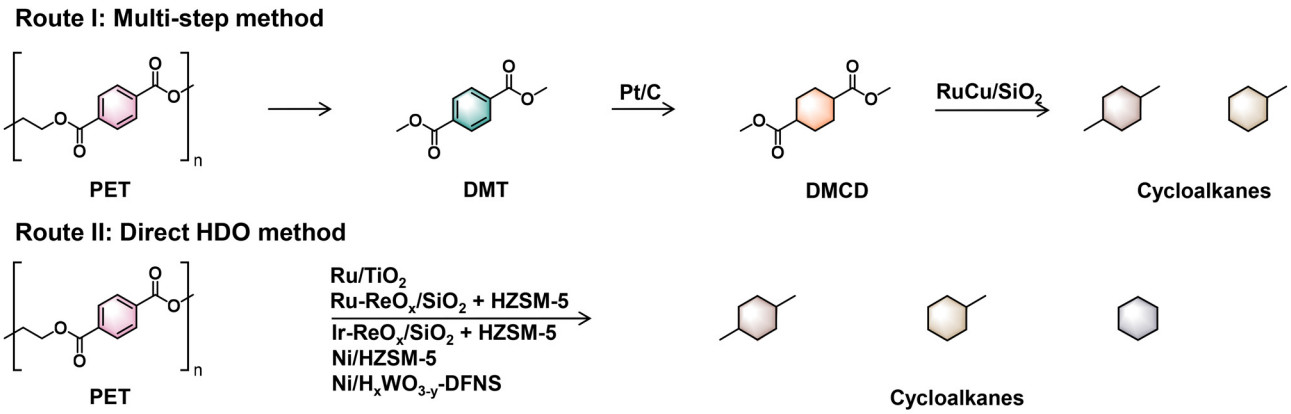

Scheme 10 Routes for the conversion of PET into cycloalkanes.

Table 6 HDO of PET over different catalysts to yield cycloalkanes

Entry	Method	Catalysts	Products	Solvent	T (°C)	P_{H_2} (MPa)	t (h)	Yield (%)	Ref.
1	Methanolysis	None	DMT	CH_3OH	200	—	3.5	97.3	96
	Hydrogenation	Pt/C	DMCD	—	140	5	10	99.2	
	HDO	Ru–Cu/SiO_2	C_7–C_8 cycloalkanes	—	400	4	8	98.4	
2	HDO	Ru/TiO_2	C_6–C_8 cycloalkanes	H_2O	200	6	10	72.9	98
3	HDO	Ru/TiO_2	C_6–C_8 cycloalkanes	H_2O + dodecane	220	6	12	90	99
4	HDO	Ru–ReO_x/SiO_2 + HZSM-5	C_6–C_8 cycloalkanes	Cyclopentane + H_2O	190	3	10	90	30
5	HDO	Ir–ReO_x/SiO_2 + HZSM-5	C_6–C_8 cycloalkanes	Cyclopentane + H_2O	190	3	4	99.5	100
6	HDO	Ni/HZSM-5	C_6–C_8 cycloalkanes	Cyclopentane	250	4	4	99	101
7	HDO	Ni/H_xWO_{3-y}-DFNS	C_6–C_8 cycloalkanes	Dodecane	280	5	16	95	102

without solvent, achieving a yield of 97.3% under conditions of 200 °C for 3.5 h. A Pd/C catalyst was utilized for the selective hydrogenation of DMT to DMCD, achieving 99.2% yield at 140 °C, 5 MPa H_2 over 7 h. In the HDO step, a novel bimetallic Ru–Cu/SiO_2 catalyst was developed. Owing to the formation of a Ru–Cu alloy, this catalyst demonstrated exceptional HDO activity, producing nearly 80% C_7–C_8 cycloalkanes. The resulting C_7–C_8 cycloalkanes can be blended with conventional bio-jet fuel to enhance fuel density and seal swelling properties.

Compared with the multi-step route, the one-pot direct conversion of PET into cycloalkanes is more economical (Scheme 9, Route II). In this context, several precious metal catalysts, including Ru/TiO_2,[98] Ru–ReO_x/SiO_2 + HZSM-5,[30] and Ir–ReO_x/SiO_2 + HZSM-5,[100] have been developed. Ru-based catalysts provided a higher yield of C_6–C_7 cycloalkanes than Ir-based catalysts due to their superior activity in C–C cracking reactions, such as decarboxylation, decarbonylation, and C–C hydrogenolysis. On the other hand, the Ir–ReO_x/SiO_2 + HZSM-5 catalyst system exhibited remarkably high selectivity for the desired DMCH product, achieving a DMCH yield of up to 95.9% under very mild reaction conditions (190 °C, 3 MPa H_2 for 4 h).

The reaction pathways for the HDO of PET to cycloalkanes over Ru/TiO_2 catalysts and bimetallic catalysts differ significantly. In the case of the Ru/TiO_2 catalyst, the initial step involves PET depolymerization to TPA intermediates.[98,99] Subsequently, TPA undergoes hydrogenation and hydrogenolysis processes to form DMCH. Additionally, decarboxylation and C–C bond hydrogenolysis during the cycloalkane methanol process yield C_6–C_7 cycloalkanes. The metal–acid bifunctionality, hydrophilicity, and high dispersion of Ru particles enable the Ru/TiO_2 catalyst to effectively facilitate PET depolymerization and cleave C–O bonds. In contrast, for the bimetallic Ir–ReO_x/SiO_2 + HZSM-5 catalyst system, the initial reaction step is the hydrogenation of PET aromatic rings.[100] Following this, depolymerization proceeds *via* the direct hydrogenolysis of acyl C–O bonds in the saturated PET segment, accompanied by cascade HDO reactions of alcoholic C–O bonds that yield C_8–ester and C_8–OH compounds. Further hydrogenolysis of the acyl C–O bond in C_8–ester leads to the formation of C_8–OH *via* an aldehyde intermediate. Finally, HDO conversion of C_8–OH produces the desired DMCH, along with concurrent C–C hydrocracking reactions that generate methylcyclohexane (MCH) and methane (Fig. 8a). The synergistic effect between ReO_x species and metallic Ir species drives the HDO of PET to cycloalkanes, wherein ReO_x species are responsible for the adsorption and activation of C–O bonds, while metallic Ir species play a critical role in hydrogen activation. Moreover, the addition of HZSM-5 zeolite accelerates the dehydration reaction step, thereby enhancing the HDO activity of the Ir–ReO_x/SiO_2 catalyst (Fig. 8b).

In the one-pot HDO process utilizing precious catalysts, the use of water as a co-solvent is essential for achieving high yields of cycloalkanes. For the Ru/TiO_2 catalyst, water plays a

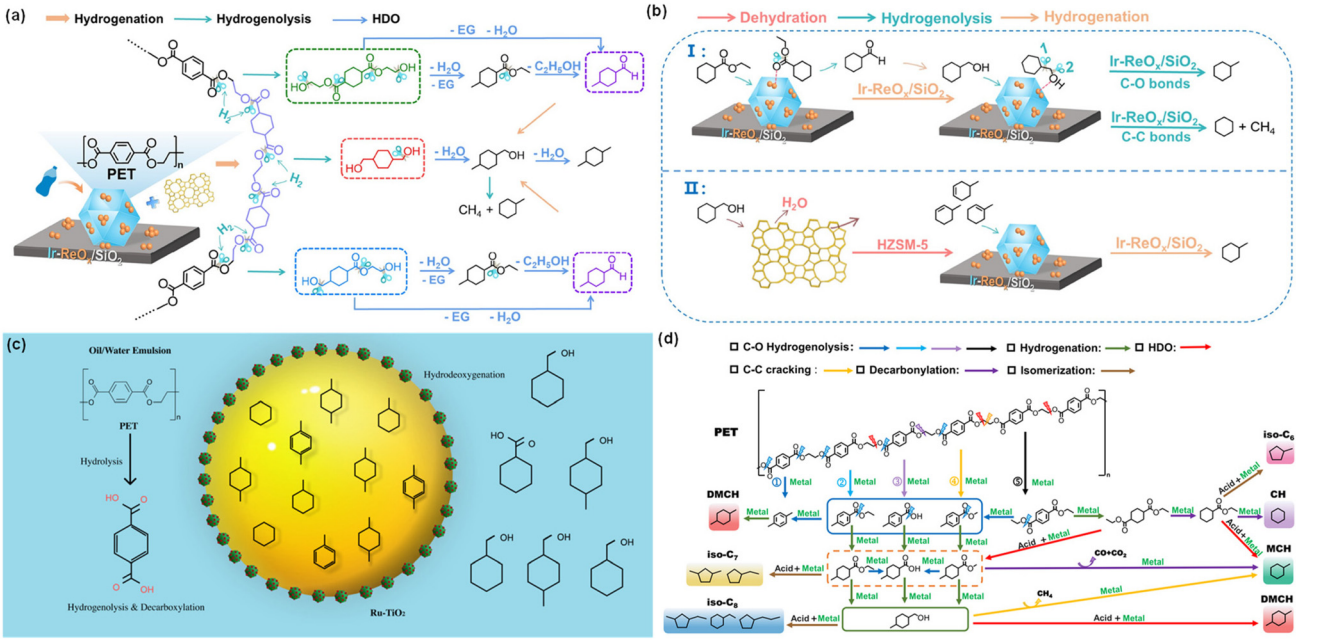

Fig. 8 (a) The reaction pathway and (b) the reaction mechanism for the HDO of PET to DMCH over Ir–ReO_x/SiO_2 + HZSM-5. Reproduced with permission.[100] Copyright 2025, Springer Nature. (c) Schematic diagram of the catalytic reaction at the oil–water interface of a stabilized Pickering emulsion droplet over Ru/TiO_2. Reproduced with permission.[99] Copyright 2025, The Royal Society of Chemistry. (d) The reaction pathway for the HDO of PET to cycloalkanes over the Ni/HZSM-5 catalyst. Reproduced with permission.[101] Copyright 2025, American Chemical Society.

critical role in the hydrolysis of PET to TPA intermediates.[98] Additionally, the presence of water facilitates the formation of a water–dodecane (O/W) biphasic system.[99] Due to the hydrophilic nature of the Ru/TiO_2 catalyst, it forms stable Pickering emulsion droplets within this biphasic system (Fig. 8c). These droplets create a large interfacial area between the oil and water phases, enhancing accessibility to the catalyst's active sites, stabilizing intermediates, improving mass transfer, and facilitating the separation of target products. Furthermore, the addition of water significantly accelerates proton transfer on the catalyst support in the biphasic system. Leveraging these advantages, the metal–acid bifunctionality, hydrophilicity, and high dispersion of Ru particles enable the catalyst to effectively cleave C–O bonds, thereby promoting the formation of C_6–C_8 cycloalkanes. For the Ru–ReO_x/SiO_2 + HZSM-5[30] and Ir–ReO_x/SiO_2 + HZSM-5 catalyst systems,[100] the hydrogenation of PET aromatic rings represents the rate-determining step during the HDO process. The presence of water enhances the hydrogenation of PET aromatic rings *via* the "on-water" mechanism; this is attributed to the protic properties of water. Consequently, high HDO activity can be achieved over these catalytic systems.

8.2 HDO of PET over non-noble Ni-based catalysts to yield cycloalkanes

To reduce the high cost associated with precious metal catalysts, our group developed a bifunctional Ni/HZSM-5 catalyst using the EG-assisted impregnation method for the direct HDO of PET to cycloalkanes.[101] A cycloalkane yield of up to 99% was achieved. Unlike noble-metal catalysts, the Ni/HZSM-5 catalyst produced a significant proportion of cycloalkanes with five-membered rings, particularly when supported on HZSM-5 with a low SiO_2/Al_2O_3 ratio. These five-membered ring cycloalkanes were formed *via* dehydration and ring isomerization reactions catalyzed by the acidic sites of HZSM-5. The reaction pathway for cycloalkane production *via* PET HDO was elucidated through time-dependent experiments involving PET HDO and related model compounds (Fig. 8d). This process primarily consists of two main stages: (1) PET depolymerization through the cleavage of C–O and C–C bonds, yielding intermediates such as methyl aromatic esters, acids, PX, and trace amounts of diethylterephthalate; and (2) subsequent conversion of these intermediates into cycloalkanes *via* HDO and hydrogenation reactions. In the depolymerization stage, acyl C–O bonds are more prone to hydrogenolysis, leading predominantly to aromatic mono-esters and PX formation, which is mainly catalyzed by Ni metallic sites. For the HDO reaction, the dual metal–acid sites of Ni/HZSM-5 cooperatively drive the reaction through dehydration and hydrogenation. Additionally, the acidic sites catalyze ring isomerization reactions, resulting in cycloalkanes with five-membered rings. The metal–acid balance (MAB) plays a critical role in determining HDO activity and product distribution. With a high MAB, HDO activity decreases due to reduced dehydration rates of cyclohexane in methanol. Furthermore, as MAB increases, the selectivity toward desired C_8 cycloalkanes and five-membered ring cycloalkanes gradually decreases; this is attributed to the high decarboxylation activity of Ni metallic sites. The catalyst can be

recycled up to five times without loss of cycloalkane yield after regeneration *via* calcination and reduction. Moreover, this catalyst demonstrates versatility in converting various PET wastes, including transparent and colored PET bottles, fibers, and even PET bottles with food residue, achieving cycloalkane yields of up to 99%. Furthermore, it enables the conversion of mixed plastics (PET + PC + PPO) into cycloalkanes with an impressive yield of 99%.

In addition to the Ni/HZSM-5 catalyst, Ouyang *et al.* developed a WO_3-incorporated dendritic fibrous nano-silica (DFNS)-supported non-noble Ni-based catalyst (Ni/H_xWO_{3-y}-DFNS) for the HDO of PET to cycloalkanes.[102] This catalyst achieves complete conversion of PET with 98.2% yield of C_6–C_8 cycloalkanes under conditions of 280 °C, 5 MPa H_2, and a reaction time of 3.5 h. The yield of the desired C_8 cycloalkane is 52.5%. The reaction pathway involves random cleavage of C–O/C–C bonds to form alkylbenzoates, which are subsequently subjected to HDO to produce cycloalkanes, alongside decarboxylation and decarbonylation pathways leading to cyclohexane and methylcyclohexane. Notably, the hydrogenolysis of the alkyl C–O bond in the ester group serves as the primary route in the initial step, differing from the mechanism observed over Ni/HZSM-5. Characterization studies revealed that the strong interaction between H_xWO_{3-y} and Ni promoted electron transfer from H_xWO_{3-y} to Ni, thereby enhancing H_2 activation and desorption and improving catalytic activity. The catalyst showed good stability, maintaining cycloalkane yields after being reused four times. Furthermore, this catalyst successfully converts waste PET bottles into cycloalkanes with a yield of 93.1%.

9 Limitations, challenges and advantages of the reductive process

The catalytic reductive process enables the conversion of PET into a wide range of valuable fuels, chemicals, and degradable polymers that cannot be obtained through traditional solvolysis depolymerization or thermal pyrolysis. The selectivity and yield of the target products are notably high, and the reaction conditions are highly mild, even allowing for solvent-free operation. Although significant progress has been made in this field, the limitations, challenges, and advantages of this process still require to be systematically addressed.

(1) Drawbacks of the current catalytic process: In the production of CHDM and MMB chemicals, the direct conversion of PET remains limited, as the current process requires multiple steps involving solvolysis depolymerization followed by hydrogenation or hydrogenolysis. Such multi-step processes are neither energy-efficient nor economically viable due to the necessity of additional high-cost separation steps. Therefore, one-pot tandem reaction technology is preferred as a means to enhance overall process efficiency. Additionally, the reductive processes predominantly employ noble metal catalysts, particularly Ru- and Pd-based systems, which significantly hinder economic viability due to their high costs. Although several non-noble metal catalysts, such as Ni- and Co-based materials, have been developed, these often suffer from deactivation issues that prevent their practical application. Accordingly, further studies on deactivation mechanisms are required, along with the development of cost-effective catalysts with high activity and stability. Moreover, simple catalyst preparation methods, such as the impregnation technique, are recommended to facilitate scalability.

(2) Practical limitations when dealing with real-world PET wastes: Real-world PET wastes often contain various additives, such as dyes, food residues, finishes, and plasticizers. It is crucial to consider the impact of these additives during the reductive conversion of PET waste. For instance, dyes are compounds containing amino groups and halogens, which can significantly affect catalyst performance, particularly in acid-catalyzed processes.[103] Indeed, the activities of HDO catalysts, such as Ru/Nb_2O_5,[95] Ru–ReO_x/SiO_2 + HZSM-5,[30] Ir–ReO_x/SiO_2 + HZSM-5,[100] and Ni/HZSM-5,[101] are notably reduced when processing PET waste containing colorants. In addition to negatively affecting catalyst activity, the presence of additives may also complicate the separation of final products, potentially lowering product quality, especially for monomers. Therefore, the separation of additives from real-world PET waste or from the final product mixtures should be carefully considered to ensure product purity. Moreover, PET is frequently used in multilayer films composed of other polymers such as polyolefins, ethylene vinyl acetate (EVA), polyvinyl chloride (PVC), and polyamide (PA).[104] Separating pure PET from such multilayer structures is highly challenging. In this context, catalyst performance may be influenced by the presence of these other polymers, particularly PVC, which can reduce process efficiency. If the catalyst is also capable of converting non-PET polymers into different products, product separation becomes an additional challenge. Therefore, catalysts with high selectivity toward PET conversion are preferred for processing multilayer films. Beyond additives and multilayer films, PET is often mixed with other plastics. Effective recycling requires appropriate sorting, as it minimizes contamination and ensures that each type of PET can be efficiently converted. Hence, technological innovations in identification and sorting methods, such as NMR-based identification and optical sorting, are needed.[105,106] With advanced sorting technologies and catalysts that exhibit high tolerance to contaminants, the reductive conversion of real-world PET plastic waste holds significant promise.

(3) The environmental impact of solvent use: Solvents play a critical role in determining the sustainability of industrial processes.[107–109] In many reported systems, toxic or high-boiling-point solvents such as dioxane and HFIP are commonly employed; these present significant challenges for large-scale and environmentally sustainable implementation. One of the most effective strategies to mitigate the environmental impact associated with solvent usage is the development of solvent-free reductive processes. For instance, the Marks' research group demonstrated the hydrogenolysis of PET into TPA using C/MoO_2[69] and Pd/C + $Hf(OTf)_4$[70] catalyst

systems under solvent-free conditions. These processes are very attractive for practical applications. Alternatively, the use of green solvents, such as water, ethanol, and supercritical fluids, offers a promising approach. Water, being the least toxic solvent, has been utilized in the reductive conversion of PET into PECHD,[26] PTA,[73] and CHDM.[36] The adoption of green solvents in place of toxic alternatives is strongly advocated to enhance the environmental sustainability and industrial feasibility of such processes. Capello *et al.* introduced a comprehensive framework for evaluating the environmental performance of solvents by integrating the assessment of substance-specific hazards with the quantification of emissions and resource consumption over the entire life cycle of a solvent.[107] This framework can serve as a guiding principle for solvent selection. Beyond environmental considerations, the efficiency of reductive reactions may strongly depend on specific solvent properties. Therefore, solvents with comparable functional properties but reduced toxicity are preferred as substitutes. For example, dioxane can be replaced with the more environmentally benign alternative 2-methyltetrahydrofuran.[110] Furthermore, mixed solvent systems, such as ethanol–water mixtures, represent another viable option, as they generally offer improved environmental profiles compared to pure alcohols.[107]

(4) Comparison with thermal pyrolysis and solvolysis depolymerization: The prevailing strategy in PET recycling involves the use of solvents to depolymerize PET into its corresponding monomers. However, this approach often faces significant challenges, including the requirement for a large excess of solvent, the reliance on homogeneous and corrosive catalysts, and difficulties in product separation. Another widely adopted method for PET conversion is thermal pyrolysis, which decomposes PET into smaller molecules such as aromatic hydrocarbons, gaseous compounds (*e.g.*, CO_2 and CO), aliphatic hydrocarbons, and solid residues at high temperatures (300–500 °C).[111–114] Nevertheless, thermal pyrolysis is an energy-intensive process. Moreover, the yield of aromatics is rather low (<40%) and product selectivity is difficult to control. Furthermore, a considerable portion of carbon remains unutilized in the form of coke. In contrast, reductive transformation methods represent a promising technology for the upcycling of PET waste into various high-value products under relatively mild reaction conditions (<300 °C). Compared to conventional approaches, reductive transformation offers several advantages, including the ability to generate a diverse range of valuable chemicals, high product selectivity, the use of heterogeneous catalysts, and operation under milder reaction conditions. For instance, the HDO of PET over a Co–Fe–Al catalyst can yield up to 99% PX at significantly lower reaction temperatures (200–220 °C).[91] The combination of mild reaction conditions and high PX yield makes this process markedly superior to thermal pyrolysis. Similarly, the hydrogenolysis of PET using C/MoO_2[69] and Pd/C + $Hf(OTf)_4$[70] catalyst systems can achieve nearly 99% yield of TPA under solvent-free reaction conditions. However, traditional hydrolysis processes typically require large quantities of solvents, which introduce significant challenges in product separation and purification. When compared to conventional methods in terms of product selectivity and energy efficiency, the reductive conversion of PET demonstrates greater environmental sustainability and practical feasibility. Nonetheless, comprehensive techno-economic analysis (TEA) and life cycle assessment (LCA) should be conducted to systematically evaluate the economic viability and environmental impact of these processes.

10 Conclusion and perspectives

Catalytic reductive recycling and upcycling of PET represents a promising strategy for producing fuels, chemicals, and degradable polymers. The catalytic reductive conversion strategies encompass hydrogenation, hydrogenolysis, HDO and transfer HDO. Depending on the extent of ring saturation, ester bond cleavage, and C–O bond removal, these reductive methods can yield various valuable products, including PECHD, PET-PECHD, CHDA, DMCD, BHCD, CHDM, TPA, MMB, p-TA, aromatics, and cycloalkanes. Various metal-based catalysts, such as Ru-, Ir-, Ni-, Co-, and Cu-based catalysts, have been employed for reductive conversion. By regulating the combination of metal and support, metal–metal oxide interactions, metal microenvironments, and acid additives, these metal-based catalysts exhibit excellent performance along each reductive pathway, achieving high yields of desired products. The relationship between catalyst structure and performance for each reductive process has been systematically discussed. Additionally, the reaction pathways and mechanisms for the reductive conversion of PET plastic waste over various catalyst systems have been addressed and compared. Although significant progress has been made in the reductive conversion of PET waste using diverse catalysts and processes, several critical considerations remain to be resolved, including the following aspects:

(1) Develop a one-pot tandem reaction strategy: In recent studies, the production of valuable chemicals such as MMB has been achieved using PET solvolysis products like DMT. However, this approach necessitates an additional PET solvolysis step, thereby compromising process efficiency. In contrast, a one-pot tandem process can significantly reduce the number of reaction and separation steps, thus enhancing the economic feasibility of PET upcycling. Indeed, the synthesis of p-TA can be accomplished *via* a one-pot tandem hydrolysis and semi-hydrogenation reaction using a PtW/MCM-48 catalyst.[73] Consequently, further research is warranted to develop one-pot tandem reaction strategies for the direct conversion of PET into target products. The one-pot tandem reaction technology can enhance process efficiency by eliminating the need for complex separation steps, thereby improving the economic viability of the process. The major technical challenges in realizing this type of reaction process lie in the development of multifunctional catalysts capable of catalyzing multiple reactions and in optimizing the reaction conditions for each individual step. The rational design principle for such multifunctional

catalysts should take into account the specific characteristics of each reaction, the requirements for active sites, and the integration of these active sites within a single catalytic system. Additionally, the optimization of reaction conditions for each step must be considered to achieve high product yields. This is essential because different reactions require distinct conditions to minimize by-product formation. In this regard, decoupling reaction conditions through one-pot multi-stage strategies represents a promising approach.

(2) Design of highly stable non-noble metal catalysts: Noble metal catalysts, particularly Ru- and Pd-based catalysts, are predominantly employed for the reductive conversion of PET. However, these noble metal catalysts are associated with high costs, thereby compromising the economic viability of the process. In this context, it is imperative to develop efficient and durable alternatives based on non-noble metals. PET is a polymer composed of ester linkages. Drawing inspiration from studies on the hydroconversion of biomass-derived lipids[115,116] and coal-derived dimethyl oxalate,[117,118] similar catalyst design principles can be applied to PET conversion. Although Cu-based catalysts have been utilized in some cases for the reductive conversion of PET into PX or CHDM, their stability remains unsatisfactory.[88,89,92] Therefore, further research is required to enhance the stability of non-noble metal catalysts. Additionally, elucidating the mechanisms of catalyst deactivation is essential, as it can provide guidance for the rational design of highly stable non-noble metal catalysts.

(3) Expand the product family from the reductive conversion of PET with a heterogeneous catalyst: While a wide range of products, including PECHD, PET-PECHD, CHDA, DMCD, BHCD, CHDM, TPA, MMB, p-TA, aromatics, and cycloalkanes, can be obtained from PET using heterogeneous catalysts, there remains a need to produce new chemicals. For instance, 1,4-benzenedimethanol (BDM) is one such product that serves as a reagent for synthesizing pesticides, pigments, and adhesives. Traditionally, BDM is produced *via* the reduction of TPA, which is generated by oxidizing petroleum-derived PX. In contrast, the reductive conversion of PET waste represents a more sustainable and environmentally friendly approach for BDM production. Indeed, some Ru-based molecular catalysts have been reported to effectively catalyze the hydrogenolysis of PET to BDM.[119,120] However, these homogeneous catalysts face challenges regarding separation and reusability. Therefore, greater attention should be directed toward developing heterogeneous catalysts capable of achieving the hydrogenolysis of PET to BDM or other novel compounds.

(4) Impact of additives: During the reductive conversion of PET waste, it is essential to consider the presence of additives commonly found in real PET waste. These additives include dyes, plasticizers, finishing agents, and others, which may influence both catalyst activity and the quality of recycled products. Specifically, dyes in PET fibers have been shown to significantly deactivate the performance of various catalysts, such as Ru/Nb_2O_5,[95] $Ru–ReO_x/SiO_2$ + HZSM-5,[30] $Ir–ReO_x/SiO_2$ + HZSM-5,[100] and Ni/HZSM-5,[101] during the HDO conversion of PET into aromatics and cycloalkanes. However, the detailed mechanism underlying this deactivation remains unclear. Recently, the Vlachos group conducted an intriguing study on the effects of additives during the pyrolysis and hydrocracking of polyolefins, revealing that the strong adsorption of additives or their small fragments is a primary cause of deactivation for recently developed catalysts used in polyolefin conversion.[121] Therefore, it is crucial to investigate the impact of additives on catalyst performance during the reductive conversion of PET and to develop efficient methods for their removal.

(5) Understand reaction pathways and mechanisms: Understanding the reaction network in reductive plastic conversion is essential for elucidating mechanisms and optimizing processes. Studies utilizing model compounds and key intermediates can provide valuable insights into evaluating the entire reaction network. However, small-sized model compounds may not always accurately reflect the behavior of large polymers, particularly during the initial depolymerization stage, due to the inherent complexity of plastic polymers. Therefore, studies involving large polymers are indispensable. In this context, precise intermediate identification becomes critical. Integration of advanced characterization techniques such as Fourier transform infrared spectroscopy (FT-IR), NMR, gel permeation chromatography (GPC), gas chromatography–mass spectrometry (GC-MS), high-performance liquid chromatography–mass spectrometry (HPLC-MS), and high-resolution mass spectrometry (HR-MS) are highly recommended. The reductive conversion of PET involves aromatic ring hydrogenation as well as the activation and cleavage of ester C–O bonds. In addition, the cleavage of ester C–O bonds may proceed *via* either the alkyl C–O bond or acyl C–O bond pathway. These reactions vary depending on the nature of the catalyst's active sites. In this context, future investigations employing integrated product analysis, *in situ* and *operando* spectroscopy techniques, along with theoretical calculations (*e.g.*, DFT calculations and molecular dynamics simulations) are crucial for identifying active sites and comprehending reaction mechanisms. Such efforts will provide valuable guidance for the rational design of highly efficient catalysts for PET valorization.

(6) Techno-economic analysis and life cycle assessment: To ensure the commercial viability of reductive upcycling of PET waste, it is essential to evaluate both economic feasibility and environmental impact. TEA and LCA serve as critical tools for comprehensively assessing and optimizing economic viability across scales—from laboratory to industrial settings—as well as environmental sustainability. However, such evaluations are rarely reported in the context of the reductive transformation of PET waste. Furthermore, a comparative analysis between traditional depolymerization and reductive transformation technologies is recommended, particularly in terms of overall economic benefits and carbon footprints.

Conflicts of interest

There are no conflicts to declare.

Abbreviations

PET	Polyethylene terephthalate
HDO	Hydrodeoxygenation
CAGR	Compound annual growth rate
TPA	Terephthalic acid
DMT	Dimethyl terephthalate
BHET	Bis(2-hydroxyethyl) terephthalate
PECHD	Polyethylene-1,4-cyclohexanedicarboxylate
PET-PECHD	Polyethylene terephthalate–polyethylene-1,4-cyclohexanedicarboxylate
CHDM	1,4-Cyclohexanedimethanol
HFIP	1,1,1,3,3,3-Hexafluro-2-propanol
MALDI-TOF MS	Matrix-assisted laser desorption ionization time-of-flight mass spectrometry
CHDA	1,4-Cyclohexanedicarboxylic acid
DMCD	Dimethyl cyclohexane 1,4-dicarboxylate
BHCD	Bis(2-hydroxyethyl) cyclohexane-1,4-dicarboxylate
PETG	Poly(ethylene terephthalate-1,4-cyclohexanedimethylene terephthalate)
PCT	Poly(1,4-cyclohexylene dimethylene terephthalate)
HMCA	4-(Hydroxymethyl)cyclohexanecarboxylic acid
MHA	4-Methylcyclohexanecarboxylic acid
CCA	Cyclohexanecarboxylic acid
EG	Ethylene glycol
TPD-MS	Temperature-programmed desorption coupled with mass spectrometry
PCTG	Poly(1,4-cyclohexylenedimethyleneterephthalate glycol)
PX	*para*-Xylene
TEA	Techno-economic analysis
CHM	Cyclohexanemethanol
MCHM	4-Methyl-1-cyclohexanemethanol
DMCH	1,4-Dimethylcyclohexane
4-MCHM	4-Methyl-1-cyclohexanemethanol
PP	Polypropylene
DFT	Density functional theory
NMR	Nuclear magnetic resonance
MMB	Methyl *p*-methyl benzoate
PTA	*p*-Toluic acid
PWA	Phosphotungstic acid
HMBA	4-(Hydroxymethyl)benzoic acid
BTX	Benzene, toluene, xylene
PS	Polystyrene
PPO	Polyphenylene oxide
PC	Polycarbonate
SMSIs	Strong metal–support interactions
DRIFTS	Diffuse reflectance infrared Fourier transform spectroscopy
XPS	X-ray photoelectron spectroscopy
LOHCs	Liquid organic hydrogen carriers
MCH	Methylcyclohexane
MAB	Metal–acid balance
DFNS	Dendritic fibrous nano-silica
BDM	1,4-Benzenedimethanol
FT-IR	Fourier transform infrared spectroscopy
GPC	Gel permeation chromatography
GC-MS	Gas chromatography–mass spectrometry
HPLC-MS	High-performance liquid chromatography–mass spectrometry
HR-MS	High-resolution mass spectrometry
LCA	Life cycle assessment
PVC	Polyvinyl chloride
EVA	Ethylene vinyl acetate
PA	Polyamide

Data availability

No primary research results, software or code have been included and no new data were generated or analysed as part of this review.

Acknowledgements

We thank the National Natural Science Foundation of China (No. 22208243 and 52276209) for financial support.

References

1 Editorial, *Nature*, 2021, **590**, 363–364.
2 S. Ahmed, *Nature*, 2023, **616**, 234–237.
3 J. E. Sonke, A. Koenig, T. Segur and N. Yakovenko, *Sci. Adv.*, 2025, **11**, eadu2396.
4 T. D. Moshood, G. Nawanir, F. Mahmud, F. Mohamad, M. H. Ahmad and A. AbdulGhani, *Curr. Res. Green Sustainable Chem.*, 2022, **5**, 100273.
5 X. Zhao, X. Wu, Q. Wang and F. Wu, *Science*, 2025, **388**, 1034–1034.
6 R. Geyer, J. R. Jambeck and K. L. Law, *Sci. Adv.*, 2017, **3**, e1700782.
7 J. Sun, J. Dong, L. Gao, Y.-Q. Zhao, H. Moon and S. L. Scott, *Chem. Rev.*, 2024, **124**, 9457–9579.
8 L. D. Ellis, N. A. Rorrer, K. P. Sullivan, M. Otto, J. E. McGeehan, Y. Román-Leshkov, N. Wierckx and G. T. Beckham, *Nat. Catal.*, 2021, **4**, 539–556.
9 C. Jehanno, J. W. Alty, M. Roosen, S. De Meester, A. P. Dove, E. Y.-X. Chen, F. A. Leibfarth and H. Sardon, *Nature*, 2022, **603**, 803–814.
10 M. Chu, W. Tu, Q. Zhang, W. Huang, J. Chen and D. Ma, *Nat. Rev. Clean Technol.*, 2025, 1–13.
11 B. T. Nicholls and B. P. Fors, *Science*, 2024, **384**, 156–157.
12 E. Plastics Europe, *An analysis of European plastics production, demand and waste data*, 2022.
13 J. Di, B. K. Reck, A. Miatto and T. E. Graedel, *Resour., Conserv. Recycl.*, 2021, **167**, 105440.
14 F. B. Insights, Polyethylene Terephthalate (PET) Market Size, Share & Industry Analysis, By Type (Virgin and Recycled), Application (Rigid Packaging, Film, Sheets &

Straps, and Others), and Regional Forecast, 2024–2032, https://www.fortunebusinessinsights.com/industry-reports/polyethylene-terephthalate-pet-market-101743.
15 N. A. Rorrer, S. Nicholson, A. Carpenter, M. J. Biddy, N. J. Grundl and G. T. Beckham, *Joule*, 2019, **3**, 1006–1027.
16 T. M. Joseph, S. Azat, Z. Ahmadi, O. M. Jazani, A. Esmaeili, E. Kianfar, J. Haponiuk and S. Thomas, *Case Stud. Chem. Environ. Eng.*, 2024, 100673.
17 S. Zhang, Q. Hu, Y.-X. Zhang, H. Guo, Y. Wu, M. Sun, X. Zhu, J. Zhang, S. Gong and P. Liu, *Nat. Sustainable*, 2023, **6**, 965–973.
18 S. Zhang, X. Zhao, X. Liu, L. Chen, L. Bai, S. Xu and Y.-Z. Wang, *Prog. Polym. Sci.*, 2025, 101958.
19 Z. Jia, L. Gao, L. Qin and J. Yin, *RSC Sustainability*, 2023, **1**, 2135–2147.
20 T. El Darai, A. Ter-Halle, M. Blanzat, G. Despras, V. Sartor, G. Bordeau, A. Lattes, S. Franceschi, S. Cassel, N. Chouini-Lalanne, E. Perez, C. Déjugnat and J. Garrigues, *Green Chem.*, 2024, 6857–6885.
21 A. Bohre, P. R. Jadhao, K. Tripathi, K. K. Pant, B. Likozar and B. Saha, *ChemSusChem*, 2023, **16**, e202300142.
22 E. Barnard, J. J. R. Arias and W. Thielemans, *Green Chem.*, 2021, **23**, 3765–3789.
23 M. Wang, Y. Li, L. Zheng, T. Hu, M. Yan and C. Wu, *Polym. Chem.*, 2024, **15**, 585–608.
24 H. Zhao, Y. Ye, Y. Zhang, L. Yang, W. Du, S. Wang and Z. Hou, *Chem. Commun.*, 2024, 13832–13857.
25 A. B. Lende, S. Bhattacharjee and C.-S. Tan, *Catal. Today*, 2022, **388**, 117–124.
26 A. B. Lende, S. Bhattacharjee and C.-S. Tan, *ACS Sustainable Chem. Eng.*, 2021, **9**, 7224–7234.
27 Z. Guo, H. Zhang, H. Chen, M. Zhang, X. Tang, M. Wang and D. Ma, *Angew. Chem.*, 2025, **137**, e202418157.
28 Z. Sun, K. Wang, Q. Lin, W. Guo, M. Chen, C. Chen, C. Zhang, J. Fei, Y. Zhu, J. Li, Y. Liu, H. He and Y. Cao, *Angew. Chem., Int. Ed.*, 2024, **63**, e202408561.
29 Y. Jing, Y. Wang, S. Furukawa, J. Xia, C. Sun, M. J. Hülsey, H. Wang, Y. Guo, X. Liu and N. Yan, *Angew. Chem., Int. Ed.*, 2021, **60**, 5527–5535.
30 J. Wei, M. Zhu, B. Liu, N. Wang, J. Liu, K. Tomishige, S. Liu and G. Liu, *Angew. Chem., Int. Ed.*, 2023, **62**, e202310505.
31 C. Berti, E. Binassi, A. Celli, M. Colonna, M. Fiorini, P. Marchese, E. Marianucci, M. Gazzano, F. Di Credico and D. J. Brunelle, *J. Polym. Sci., Part B:Polym. Phys.*, 2008, **46**, 619–630.
32 L. Wang, Z. Xie, X. Bi, X. Wang, A. Zhang, Z. Chen, J. Zhou and Z. Feng, *Polym. Degrad. Stab.*, 2006, **91**, 2220–2228.
33 Y. Hu, Z. Zhao, Y. Liu, G. Li, A. Wang, Y. Cong, T. Zhang, F. Wang and N. Li, *Angew. Chem., Int. Ed.*, 2018, **57**, 6901–6905.
34 K. Wang, J. Shen, Z. Ma, Y. Zhang, N. Xu and S. Pang, *Polymers*, 2021, **13**, 452.
35 T. Chen, W. Zhang and J. Zhang, *Polym. Degrad. Stab.*, 2015, **120**, 232–243.
36 S. Fang, Z. Gao, X. Shi, M. Zhang, W. Zhang and Y. Liu, *Sci. China:Chem.*, 2025, 1–9.
37 H. Chen, Z. Guo, X. Liang, M.-Q. Zhang, M. Wang and D. Ma, *ACS Catal.*, 2025, **15**, 6287–6295.
38 F. Zhang, J. Chen, P. Chen, Z. Sun and S. Xu, *AIChE J.*, 2012, **58**, 1853–1861.
39 J. Chen, L. Guo and F. Zhang, *Catal. Commun.*, 2014, **55**, 19–23.
40 L. Yan, Y. Shen, Z. Zou, X. Zhang, Z. Yu, G. Wang and C. Chen, *Inorg. Chem. Front.*, 2024, **11**, 3285–3295.
41 W. Yu, S. Bhattacharjee, W.-Y. Lu and C.-S. Tan, *ACS Sustainable Chem. Eng.*, 2020, **8**, 4058–4068.
42 J. Chen, X. Liu and F. Zhang, *Chem. Eng. J.*, 2015, **259**, 43–52.
43 H. Jia, Z. Yang, X. Yun, X. Lei, X. Kong and F. Zhang, *Ind. Eng. Chem. Res.*, 2019, **58**, 22702–22708.
44 Y. Huang, Y. Ma, Y. Cheng, L. Wang and X. Li, *Ind. Eng. Chem. Res.*, 2014, **53**, 4604–4613.
45 Q. Fan, X. Li, Z. Yang, J. Han, S. Xu and F. Zhang, *Chem. Mater.*, 2016, **28**, 6296–6304.
46 H. Xiao, C. Zhang, J. Zhao, Z. Zheng and Y. Li, *RSC Adv.*, 2023, **13**, 16363–16368.
47 W. Ren, C. Gang, C. Zhao, P. Wu and X. Li, *Appl. Catal., A*, 2025, **698**, 120233.
48 Y. Li, M. Wang, X. Liu, C. Hu, D. Xiao and D. Ma, *Angew. Chem.*, 2022, **134**, e202117205.
49 Y. Huang, Y. Si, X. Guo, C. Qin, Y. Huang, L. Wang, X. Gao, S. Yao and Y. Cheng, *ACS Catal.*, 2025, **15**, 4570–4578.
50 W. Ou, Y. Ye, Y. Zhang, H. Zhao, W. Du and Z. Hou, *Chin. J. Catal.*, 2025, **71**, 363–374.
51 S. Mo, J. Kou, J. Zeng, K. Song, Y. Zhang, S. He, Y. Hu, Y. Guo, X. Liu, X. Chen and Y. Wang, *Chem. Eng. J.*, 2024, **500**, 157249.
52 Z. Zhao, G. Gao, Y. Xi, J. Wang, P. Sun, Q. Liu, C. Li, Z. Huang and F. Li, *Nat. Commun.*, 2024, **15**, 8444.
53 X. Guo, J. Xin, X. Lu, B. Ren and S. Zhang, *RSC Adv.*, 2015, **5**, 485–492.
54 W. Ou, H. Wang, Y. Ye, H. Zhao, Y. Zhang and Z. Hou, *J. Hazard. Mater.*, 2024, **476**, 134964.
55 A. B. Hungria, R. Raja, R. D. Adams, B. Captain, J. M. Thomas, P. A. Midgley, V. Golovko and B. F. Johnson, *Angew. Chem., Int. Ed.*, 2006, **45**, 4782–4785.
56 G. Lewandowski, A. Wroblewska and E. Milchert, *Polimery*, 2007, **52**, 39–43.
57 X. Gong, M. Wang, H. Fang, X. Qian, L. Ye, X. Duan and Y. Yuan, *Chem. Commun.*, 2017, **53**, 6933–6936.
58 S. Zhang, G. Fan and F. Li, *Green Chem.*, 2013, **15**, 2389–2393.
59 H. Liu, Q. Hu, G. Fan, L. Yang and F. Li, *Catal. Sci. Technol.*, 2015, **5**, 3960–3969.
60 Z. Chang, B. Ye, Z. Zhong, S. Wang, H. Wang, W. Du and Z. Hou, *J. Mater. Chem. A*, 2024, **12**, 1003–1011.
61 X. Jiang, Z. Chang, L. Yang, W. Du and Z. Hou, *Fuel*, 2024, **363**, 130944.
62 X. Li, Z. Sun, J. Chen, Y. Zhu and F. Zhang, *Ind. Eng. Chem. Res.*, 2014, **53**, 619–625.

63 X. Xiao, H. Xin, Y. Qi, C. Zhao, P. Wu and X. Li, *Appl. Catal., A*, 2022, **632**, 118510.
64 W. Liu, Z. Wang, H. Ban, C. Tang, L. Zhang, B. Lu, K. Zhang, S. Mao and Y. Wang, *Appl. Catal. B: Environ. Energy*, 2025, 125466.
65 R. Zhang, H. Jin, L. Ma and S. Yang, *RSC Adv.*, 2023, **13**, 27036–27045.
66 R. Zhang, H. Jin, L. Ma, S. Yang and G. He, *Catal. Commun.*, 2024, **187**, 106887.
67 D. Hou, J. Xin, X. Lu, X. Guo, H. Dong, B. Ren and S. Zhang, *RSC Adv.*, 2016, **6**, 48737–48744.
68 P. Wu, G. Lu and C. Cai, *Green Chem.*, 2021, **23**, 8666–8672.
69 Y. Kratish, J. Li, S. Liu, Y. Gao and T. J. Marks, *Angew. Chem.*, 2020, **132**, 20029–20033.
70 Y. Kratish and T. J. Marks, *Angew. Chem., Int. Ed.*, 2022, **61**, e202112576.
71 W. Zeng, Y. Zhao, F. Zhang, R. Li, M. Tang, X. Chang, Y. Wang, F. Wu, B. Han and Z. Liu, *Nat. Commun.*, 2024, **15**, 160.
72 J. Cheng, J. Xie, Y. Xi, X. Wu, R. Zhang, Z. Mao, H. Yang, Z. Li and C. Li, *Angew. Chem., Int. Ed.*, 2024, **63**, e202319896.
73 Y. Zhu, Z. Mao, W. Wu, B. Han and Q. Mei, *J. Am. Chem. Soc.*, 2025, **147**, 10662–10677.
74 X. Zhao, F. Wang, X.-P. Kong, R. Fang and Y. Li, *J. Am. Chem. Soc.*, 2021, **143**, 16068–16077.
75 A. G. A. Sá, A. C. de Meneses, P. H. H. de Araújo and D. de Oliveira, *Trends Food Sci. Technol.*, 2017, **69**, 95–105.
76 J.-Z. Li, Y. Wang, W. Zeng and S.-Y. Qin, *Supramol. Chem.*, 2008, **20**, 249–254.
77 F. Yang, J. Sun, R. Zheng, W. Qiu, J. Tang and M. He, *Tetrahedron*, 2004, **60**, 1225–1228.
78 H. Liu, G. Chen, H. Jiang, Y. Li and R. Luque, *ChemSusChem*, 2012, **5**, 1892–1896.
79 J. D. Tibbetts, D. Russo, A. A. Lapkin and S. D. Bull, *ACS Sustainable Chem. Eng.*, 2021, **9**, 8642–8652.
80 T. Pfennig, R. L. Johnson and B. H. Shanks, *Green Chem.*, 2017, **19**, 3263–3271.
81 S. Chavan, S. Halligudi, D. Srinivas and P. Ratnasamy, *J. Mol. Catal. A: Chem.*, 2000, **161**, 49–64.
82 P. Raghavendrachar and S. Ramachandran, *Ind. Eng. Chem. Res.*, 1992, **31**, 453–462.
83 M. Ye, Y. Li, Z. Yang, C. Yao, W. Sun, X. Zhang, W. Chen, G. Qian, X. Duan and Y. Cao, *Angew. Chem.*, 2023, **135**, e202301024.
84 V. Murali, H. Kim, H. U. Kim, J. R. Kim, S. H. Son, Y.-K. Park, J.-M. Ha and J. Jae, *Green Chem.*, 2025, 2203–2219.
85 S. Hongkailers, Y. Jing, Y. Wang, N. Hinchiranan and N. Yan, *ChemSusChem*, 2021, **14**, 4330–4339.
86 X. Zhao, H. Wang, Z. Fang, Z. Ma, S. Sun, D. Wu, Y. Zhang, C. C. Xu, S. Lu, R. Nie and J. Fu, *Green Chem.*, 2025, 7254–7262.
87 M. Zhang, Z. Huo, L. Li, Y. Ji, T. Ding, G. Hou, S. Song and W. Dai, *ChemSusChem*, 2025, **18**, e202402013.
88 Z. Gao, B. Ma, S. Chen, J. Tian and C. Zhao, *Nat. Commun.*, 2022, **13**, 3343.
89 R. Helmer, S. S. Borkar, A. Li, F. Mahnaz, J. Vito, M. Bishop, A. Iftakher, M. F. Hasan, S. Rangarajan and M. Shetty, *Angew. Chem.*, 2025, **137**, e202416384.
90 J. Li, Z. An, Y. Kong, L. Zhang, J. Yang, X. Wang, J. Wang, D. Duan, Q. Zhang and R. Long, *Appl. Catal. B: Environ. Energy*, 2024, **357**, 124307.
91 Y. Shao, M. Fan, K. Sun, G. Gao, C. Li, D. Li, Y. Jiang, L. Zhang, S. Zhang and X. Hu, *Green Chem.*, 2023, **25**, 10513–10529.
92 Y. Shao, L. Kong, M. Fan, K. Sun, G. Gao, C. Li, L. Zhang, S. Zhang, Y. Wang and X. Hu, *ACS Sustainable Chem. Eng.*, 2024, **12**, 3818–3830.
93 M. Golubeva, M. Mukhtarova, A. Sadovnikov and A. Maximov, *Polymers*, 2023, **15**, 2248.
94 Q. Zou, T. Long, R. Fang, X. Zhao, F. Wang and Y. Li, *Angew. Chem., Int. Ed.*, 2025, e202507309.
95 S. Lu, Y. Jing, B. Feng, Y. Guo, X. Liu and Y. Wang, *ChemSusChem*, 2021, **14**, 4242–4250.
96 H. Tang, N. Li, G. Li, A. Wang, Y. Cong, G. Xu, X. Wang and T. Zhang, *Green Chem.*, 2019, **21**, 2709–2719.
97 M. Zhu, G. Hou, C. He, S. Liu and G. Liu, *React. Chem. Eng.*, 2024, **9**, 2367–2379.
98 R. Li, W. Zeng, R. Zhao, Y. Zhao, Y. Wang, F. Zhang, M. Tang, Y. Wang, X. Chang and F. Wu, *Nano Res.*, 2023, **16**, 12223–12229.
99 V. Murali, J. R. Kim, Y.-K. Park, J.-M. Ha and J. Jae, *Green Chem.*, 2023, **25**, 8570–8583.
100 N. Wang, J. Liu, J. Wei, S. Liu and G. Liu, *Sci. China: Chem.*, 2025, **68**, 1563–1575.
101 J. Liu, N. Wang, S. Liu and G. Liu, *JACS Au*, 2024, **4**, 4361–4373.
102 W. Zhong, J. Wang, X. Li, S. Wang, H. Tan and X. Ouyang, *Green Chem.*, 2025, **27**, 4621–4631.
103 E. Andini, P. Bhalode, E. Gantert, S. Sadula and D. G. Vlachos, *Sci. Adv.*, 2024, **10**, eado6827.
104 P. Tamizhdurai, V. Mangesh, S. Santhosh, R. Vedavalli, C. Kavitha, J. K. Bhutto, M. A. Alreshidi, K. K. Yadav and R. Kumaran, *J. Cleaner Prod.*, 2024, **447**, 141403.
105 J.-P. Lange, *ACS Sustainable Chem. Eng.*, 2021, **9**, 15722–15738.
106 M.-Q. Zhang, Y. Zhou, R. Cao, S. Tian, Y. Jiao, Z. Guo, M. Wang, H. Peng, B. Sun and B. Xu, *Nature*, 2025, 1–9.
107 C. Capello, U. Fischer and K. Hungerbühler, *Green Chem.*, 2007, **9**, 927–934.
108 P. G. Jessop, *Green Chem.*, 2011, **13**, 1391–1398.
109 V. Hessel, N. N. Tran, M. R. Asrami, Q. D. Tran, N. V. D. Long, M. Escribà-Gelonch, J. O. Tejada, S. Linke and K. Sundmacher, *Green Chem.*, 2022, **24**, 410–437.
110 C. Castiello, P. Junghanns, A. Mergel, C. Jacob, C. Ducho, S. Valente, D. Rotili, R. Fioravanti, C. Zwergel and A. Mai, *Green Chem.*, 2023, **25**, 2109–2169.
111 J. Cao, X. Qiu, F. Zhang and S. Fu, *ChemSusChem*, 2025, **18**, e202402100.

112 J. Lee, E. E. Kwon, S. S. Lam, W.-H. Chen, J. Rinklebe and Y.-K. Park, *J. Cleaner Prod.*, 2021, **321**, 128989.
113 Y. Liu, W. Fu, T. Liu, Y. Zhang and B. Li, *J. Anal. Appl. Pyrolysis*, 2022, **161**, 105414.
114 S. Al-Salem, A. Antelava, A. Constantinou, G. Manos and A. Dutta, *J. Environ. Manage.*, 2017, **197**, 177–198.
115 S. Xing, J. Fu, M. Li, G. Yang and P. Lv, *Renewable Sustainable Energy Rev.*, 2024, **200**, 114459.
116 S. Chen, C. Fan, Z. Liao, J. Zeng, H. Xie, H. Gong and G. Zhou, *ACS Sustainable Chem. Eng.*, 2024, **12**, 14571–14589.
117 L. Liu, J. Lu, Y. Yang, W. Ruettinger, X. Gao, M. Wang, H. Lou, Z. Wang, Y. Liu and X. Tao, *Science*, 2024, **383**, 94–101.
118 L. Liu, J. Lu, M. Liu, H. Wang, J. Zhang, G. Xu, Z. Wang, Y. Liu, J. Liang and X. Gao, *CCS Chem.*, 2025, 1–12.
119 S. Dolai, C. K. Behera and S. K. Patra, *Dalton Trans.*, 2025, 3977–4012.
120 S. Westhues, J. Idel and J. Klankermayer, *Sci. Adv.*, 2018, **4**, eaat9669.
121 J. Ngu, S. Najmi, E. Selvam, B. Vance, P. Yang and D. G. Vlachos, *Nat. Chem. Eng.*, 2025, 1–9.